Original Research Paper

A comparative evaluation of design factors on bubble column operation in photosynthetic biogas upgrading

Archishman Bose[1,2], Richard O'Shea[1,2,*], Richen Lin[1,2], Jerry D. Murphy[1,2]

[1]Environmental Research Institute, MaREI Centre, University College Cork, Cork, Ireland.

[2]School of Engineering, University College Cork, Cork, Ireland.

HIGHLIGHTS

➢Multiple factors and their interaction influence photosynthetic biogas upgrading.

➢pH and liquid to gas flow (L/G) ratio affect CO_2 removal the most.

➢Interaction between pH and L/G ratio has the highest influence on CO_2 removal.

➢L/G ratio, followed by algal concentration has the highest influence on O_2 stripping.

➢Bubble column operation predicted to produce grid quality biomethane.

GRAPHICAL ABSTRACT
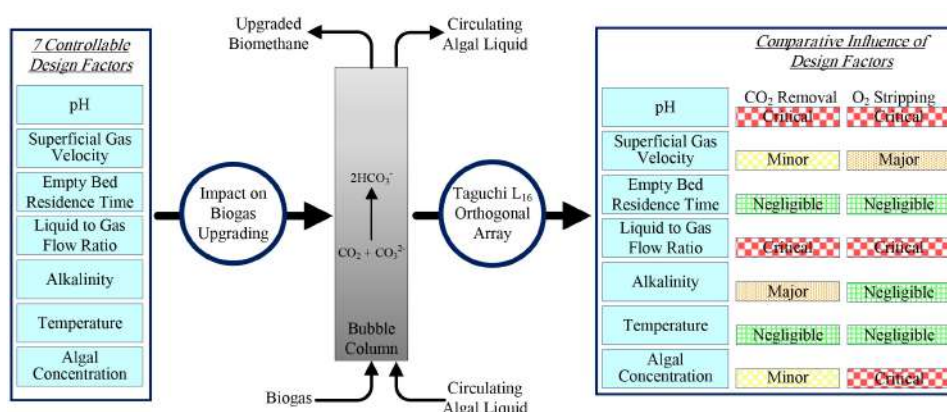
ARTICLE INFO

ABSTRACT

Studies attempting to optimise photosynthetic biogas upgrading by simultaneous investigation of the bubble column-photobioreactor setup have experienced considerable variability in results and conclusions. To identify the sources of such variation, this work quantitatively compared seven design factors (superficial gas velocity; liquid to gas flow rate (L/G) ratio; empty bed residence time; liquid inlet pH; liquid inlet alkalinity; temperature; and algal concentration) using the L_{16} Taguchi orthogonal array as a screening design of experiment. Assessments were performed using the signal to noise (S/N) ratio on the performance of CO_2 removal (CO_2 removal efficiency, CO_2 absorption rate, and overall CO_2 mass transfer coefficient) and O_2 stripping (O_2 concentration in biomethane and O_2 flow rate in biomethane). Results showed that pH and L/G ratio were the most critical design factors. Temperature and gas residence times had minimal impact on the biomethane composition. The interactive effect between pH and L/G ratio was the most impactful, followed by the interactive effects between superficial gas velocity and L/G ratio and pH on CO_2 removal efficiency. The impact of L/G ratio, algal concentration, and pH (in that order of impact) caused up to a 90% variation in oxygen content in biomethane. However, algal concentration had a diminishing role as the L/G ratio increased. Using only the statistically significant main effects and interactions, the biomethane composition (CO_2% and O_2%) was predicted with over 95% confidence through regression equations for superficial gas velocity up to 0.2 cm/s.

* Corresponding author at: Tel.: +353 21 490 1971
E-mail address: richard.oshea@ucc.ie

Contents

Abbreviations and Nomenclatures

Adj	Adjusted	n_{ex}	Number of experiments
Alk	Alkalinity (g-IC/L)	OA	Orthogonal array
ANOVA	Analysis of variance	PI	Prediction interval
C_{alg}	Algae concentration (g-DW/L)	R_{abs,CO_2}	Mean steady state CO_2 absorption rate (mol/L/s)
CI	Confidence interval	R_{eff,CO_2}	Efficiency of CO_2 removal from biogas (%)
DoF	Degree of freedom	SB	Smaller-the-better
DW	Dry weight	S/N	Signal to noise
EBRT	Empty bed residence time (min)	SS	Sum of squares
G	Biogas flow rate (mLn/s)	SSE	Sum of square errors
IC	Inorganic carbon	T_{col}	Temperature of bubble column (°C)
k	kilo	TRL	Technology readiness level
$k_{G_{CO_2}}a$	Mean overall CO_2 mass transfer coefficient (h^{-1})	u_G	Superficial gas velocity (cm/s)
LB	Lower-the-better		
L/G	Liquid to gas flow rate (L/G) ratio	**Subscripts**	
mL_n	Milli-litres normal	BC	Bubble column
MS	Mean squares	BG	Biogas
N	Molar flow rate (mol/s)	BM	Biomethane

1. Introduction

1.1. Microalgal (photosynthetic) biogas upgrading

Biomethane from anaerobic digestion (AD) is a renewable and versatile biofuel (Rajendran et al., 2019; Wall et al., 2017). Compared to conventional biogas upgrading technologies such as water scrubbing and pressure swing absorption, novel biogas upgrading technologies aim to increase the sustainability of biomethane derived from biogas by reducing costs and energy demands (Angelidaki et al., 2018). The two-step photosynthetic biogas upgrading process, employing CO_2 removal and subsequent utilisation of CO_2 by microalgae, is considered a novel biogas upgrading technology (Meier et al., 2015; Bose et al., 2019). In the first step, as shown in **Figure 1**, CO_2, as well as H_2S are absorbed in a bubble column by a carbonate-rich sodium carbonate-bicarbonate buffer solution (pH 9 and above) *via* the principle governing **Equation 1** (Bose et al., 2019), decreasing the pH. In the subsequent step, the bicarbonate uptake by the algae in a photobioreactor regenerates carbonate in the solution with a corresponding rise in pH (**Equation 2**). The re-circulation of the regenerated carbonate-rich solution into the bubble column then continues the carbonate-bicarbonate cycle. In addition to the biomethane, the cultivated microalgae is a high-value product critical to improving both the economic benefits and sustainability of the biomethane produced (Bose et al., 2020).

Bubble Column: $CO_2 + H_2O + CO_3^{2-} \rightarrow 2HCO_3^-$ Eq. 1

Photobioreactor: $\begin{cases} HCO_3^- \xrightarrow{\;Algae\;} CO_2 + OH^- \\ HCO_3^- + OH^- \xrightarrow{\;Medium\;} CO_3^{2-} + H_2O \end{cases}$ Eq. 2
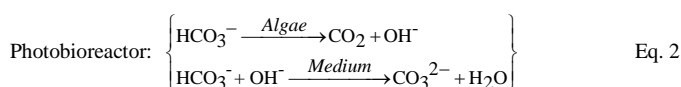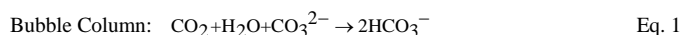
1.2. Need for a focussed approach to photosynthetic biogas upgrading

Ensuring continuous grid-quality biomethane (CO_2 and O_2 less than 2.5% and 1% by volume, respectively) (Meier et al., 2017; Gas Networks Ireland, 2018) and adequate carbon uptake by microalgae is essential to maximise the economic and environmental benefits from the photosynthetic biogas

upgrading system. To achieve this, the influence of multiple operational factors (compiled in **Table 1**) such as pH (Bahr et al., 2014; Bose et al., 2019), gas and liquid flow velocities (Bose et al., 2019; Meier et al., 2019) and flow rates (Toledo-Cervantes et al., 2017), temperature (del Rosario Rodero et al., 2018), alkalinity (del Rosario Rodero et al., 2018 and 2020b), biogas composition (Bose et al., 2019), the concentration of the algae (Bose et al., 2019; del Rosario Rodero et al., 2020b), as well as the microalgae species and its cultivation conditions (Bose et al., 2019) must be simultaneously taken into account. Accordingly, the operations of the individual components in photosynthetic biogas upgrading such as the bubble column and the microalgae cultivation and harvesting systems could significantly deviate from those of optimised stand-alone setups. For example, when *Spirulina platensis* is chosen as the microalgae, the bubble column in the photosynthetic biogas upgrading system should operate below a pH of 11 and a temperature of 40 °C to prevent severe damage to the microalgae (De Oliveira et al., 1999). This is in contrast to operating conditions of pH above 11 and a temperature above 40 °C, commonly employed for CO_2 removal in an alkaline medium without the presence of microalgae (Knuutila et al., 2010). In another example of differentiation between individual components and the integrated system, researchers aimed to achieve a carbon balance in the bubble column-photobioreactor system by fixing algal productivity (Marín et al., 2021). The controlled values varying between 7.5-15 $g/m^2/d$ were much lower than the achievable productivity of 20-25 $g/m^2/d$ in open pond systems (Sun et al., 2016).

The simultaneous influence of multiple design factors and their corresponding levels of operation on photosynthetic biogas upgrading (compiled in **Table 1**) could be seen to generate variability in conclusions on the system performance. For instance, Toledo-Cervantes et al. (2017) suggested the use of co-current bubble column configuration and a liquid to gas flow rate (L/G) ratio of less than 1 to achieve grid-quality biomethane. However, del Rosario Rodero et al. (2020a), employing a counter-current bubble column, reported 14.1% CO_2 concentration in upgraded biomethane at an L/G ratio of 0.8 in a pilot-scale facility. In a more recent study, the CO_2 content in the biogas varied between 1.5% and 4.4% at an alkalinity of 1200 mg/L inorganic carbon (IC) and inlet pH between 9.7 and 9.8 (del Rosario Rodero et al., 2020b). In contrast, Marín et al. (2021), in a similar experimental range and using a similar setup, reported a much lower CO_2 content in biogas of 0.5%. Seasonal variations,
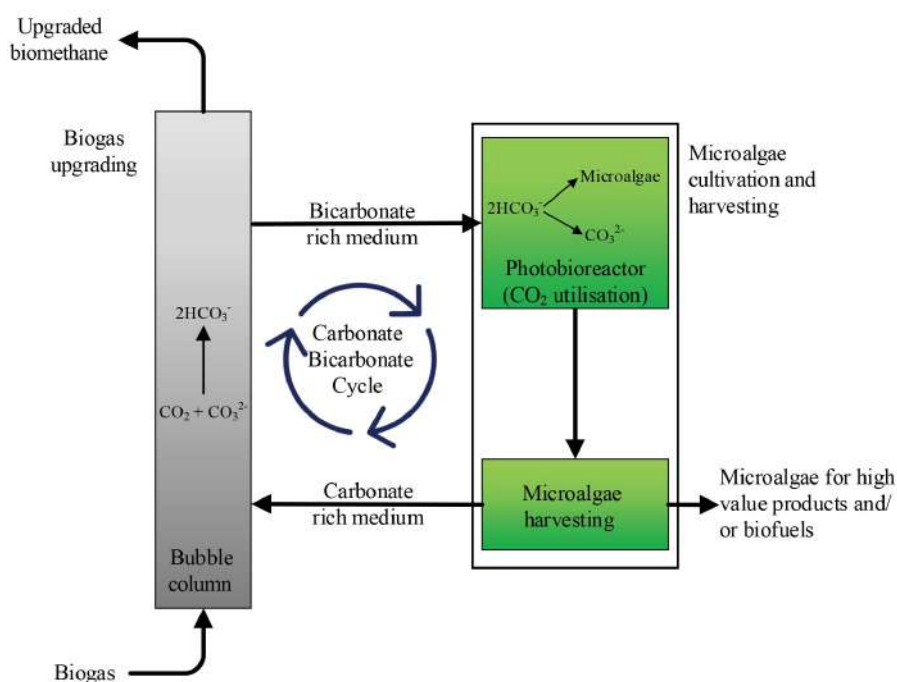
Fig. 1. Diagrammatic representation of the two-step bubble column-photobioreactor photosynthetic biogas upgrading system using the carbonate bicarbonate cycle for the production of biomethane and microalgae for high-value products and/or biofuels.

Table 1.
Variables affecting bubble column operations in photosynthetic biogas upgrading including those selected in the present study for comparative assessment. The current and limiting/industrial level have been compiled from multiple literature sources*.

Variables	Description	Levels			Factor selection in current study
		Current	**Limits/Levels**	**Research need**	
Superficial gas velocity (cm/s)	Inlet velocity of biogas to the bubble column	0.05 – 0.5	4	To be increased	Selected
Empty bed residence time (min)	Time of biogas in an empty bubble column, indicating the height of the column	10-90	3-6	To be reduced	Selected
Aspect ratio	Ratio of column height to diameter	10-110	3-10 (Jakobsen, 2009)	To be reduced	Not selected as confounded with the both the previous factors
L/G ratio	Ratio of liquid to gas flow rate	0.5-10	NA	To be optimised	Selected
Flow configuration	Co-current or counter current gas-liquid flow configurations	Co/Counter current	NA	N/A	Co-current chosen after Toledo-Cervantes et al. (2017)
pH	pH of the algal solution at the bubble column inlet	7-10.5	8.5-11	To be optimised	Selected
Alkalinity (g-IC/L)	Strength of a buffer solution, indicating the amount of dissolved inorganic carbon content in solution	0.1-4.1	N/A	To be optimised	Selected
Temperature (°C)	Operating temperature of bubble column	10 - 28	20 - 40	To be optimised	Selected
Algae concentration (g-DW/L)	Concentration of microalgae in cultivation medium	Algae circulated after harvesting	Up to 10 (Huang et al., 2017)	To be optimised	Selected
Light (klux)	Cool white light affecting appreciable *Spirulina platensis* growth	On/Off	As per those required by chosen algal species	Effect to be understood	Kept on at all times in the bubble column setup
Algae productivity (g-DW/L/d)	Average daily growth rate of microalgae	0.06-0.1	0.175 (De Oliveira et al., 1999)	To be maximised	Not considered as not directly linked to bubble column optimisation
CO_2 in biogas (%)	CO_2 concentration in the influent biogas	NA	20-55	External factor	Kept constant as an external factor
H_2S in biogas (ppm)	H_2S concentration in the influent biogas	NA	0-10,000	External factor	
Dissolved oxygen (DO) concentration (mg/L)	The content of the dissolved oxygen in the inlet algal liquid	2-15	<100% air saturation level (Molina et al., 2001)	External factor	Kept constant as an external factor

NA: Not applicable; IC: Inorganic carbon; DW: Dry weight

* Sources: Bahr et al. (2014), Posadas et al. (2015a and b), Franco-Morgado et al. (2017), Meier et al. (2017), Toledo-Cervantes et al. (2017), Marín et al. (2018 and 2021), Bose et al. (2019), del Rosario Rodero et al. (2018, 2019a and b, 2020a and b)

especially with open pond microalgae cultivation caused CO_2 percentages in biomethane to vary from 0.7% during summer to 11.9% during winter; the corresponding O_2 concentration varied between 0% and 3.5% (Marín et al., 2018). Diurnal variations between 2% and 4.5% in CO_2 content in the upgraded biomethane were reported by Meier et al. (2017).

These variabilities and uncertainties arise not only from the different experimental conditions that exist in each study but also from the probable interactive effects among operating factors that are seldom assessed in studies. Present Technology Readiness Levels (TRLs) would suggest viable knowledge for scale-up and industrial-scale implementation of photosynthetic biogas upgrading but would still suffer from significant uncertainty. Therefore, rather than trying to optimise the overall photosynthetic biogas upgrading system, a focused look into individual sub-systems could be beneficial. It would allow optimisation of biogas upgrading and hence the selection of appropriate microalgae cultivation and harvesting techniques to maximise the overall system effectiveness and robustness.

1.3. Objective and novelty

Research on bubble columns for CO_2 absorption in sodium/potassium carbonate-bicarbonate solutions has primarily focused on performance improvement in either pure or catalysed solutions in the absence of microalgae (Knuutila et al., 2010; Hu et al., 2016). On the contrary, microalgae cultivation (Vasumathi et al., 2012; Huang et al., 2017) and harvesting (Barros et al., 2015; Singh and Patidar, 2018) have been extensively studied and discussed in the literature under similar conditions suitable for photosynthetic biogas upgrading.

Thus, in a novel approach, rather than optimisation by varying a few factors, the present work aims to compare the main effects of, and interactions between, different design factors on the bubble column performance for biogas upgrading. The Taguchi orthogonal array (OA) as screening design of experiment was selected as the statistical tool. Using this comparative assessment, the authors believe a significant knowledge gap in the operation of the bubble column and hence the overall photosynthetic biogas upgrading system could be overcome. Accordingly, experiments were conducted on a lab-scale bubble column to:

i. determine and rank the factors according to their influence on the performance of the bubble column for photosynthetic biogas upgrading;
ii. determine the most impactful interactive effects between the design factors in affecting the bubble column operations
iii. identify the suitable operating setpoints of the design factors to ensure robust operation of the bubble column
iv. predict and analyse the operation of the bubble column with respect to product biomethane composition and its significance to photosynthetic biogas upgrading.

2. Materials and Methods

2.1. Microorganisms and culture conditions

All experiments were performed with microalgae *Arthrospira* (Spirulina) *platensis* SAG 85.79, from Sammlung von Algenkulturen Goettingen (SAG), Germany. The microalgae were grown in 3-L batches

within 5-L Erlenmeyer Flasks with continuous bubbling of air. Temperature and light were maintained at 20 ± 1 °C and 4000 ± 500 lux with a 16:8 light/dark cycle. Modified Zarrouk's medium was used as the nutrient medium, the detailed composition of which can be found elsewhere (Madkour et al., 2012). The cultures were transferred to a new medium every three to four weeks to continue cultivation. Strains were maintained in 100 mL Erlenmeyer flasks, maintaining a pH between 9 and 10.

2.2. Experimental setup

Experiments were conducted in a 2-m high, 24-mm diameter absorption (bubble) column made from a clear acrylic tube of the same dimensions. Multiple liquid outlets at desired heights were fitted to allow the study of variable gas flow rates and empty bed residence time (EBRT). A 24-mm diameter, 300-mm high gas liquid separator was used to remove all trapped gas bubbles at the liquid outlet. The entire setup was housed in a cabinet capable of maintaining temperature and light intensities between 20 to 40 °C and 2000 to 6000 lux, respectively. A schematic overview of the experimental setup is provided in **Figure 2**.

The microalgae solution was pumped through the bottom of the column by a VWR® AU-UPC-EZ programmable peristaltic pump in a co-current configuration to the biogas. Synthetic biogas, at an absolute pressure of 1.2 bar was bubbled through a 25-mm long and 18-mm diameter air-stone diffuser placed at the bottom of the bubble column. Synthetic biogas comprising 40% CO_2 and the remainder N_2 (in lieu of CH_4) without any H_2S was chosen from safety considerations. N_2 in lieu of CH_4 has been previously used in literature (Posadas et al., 2015a) due to its inertness and similar solubility (0.0019 g/100g H_2O) to that of CH_4 (0.0023 g/100 g H_2O) (Kaye and Laby, 1986) under atmospheric conditions. The individual N_2 and CO_2 flows were controlled by separate flow controllers (Red-y smart controller GSC, Vögtlin Instruments® GmbH). Differential pressure between the top of the bubble column and the atmosphere fluctuated between 0.01 ± 0.01 bar (g) measured by a manometer fitted to the outlet of the column.

The liquid outlet from the gas/liquid separator was routed to a tee with one end open to the atmosphere *via* a U-shaped connection, as shown in **Figure 2**. This prevented the syphoning out of the liquid from the gas-liquid separator while allowing the outlet flow to match the inlet flow controlled by the peristaltic pump. The combined outlet gas from the bubble column and the gas liquid separator were sequentially routed through a foam trap and an ice bath to remove foam and moisture. Inside the ice bath, a larger pipe diameter pipe was used as a condensate trap and was regularly drained after a few experiments to ensure its adequacy of operation. Flow and composition measurements were hence performed on a dry gas basis as described in *Section 2.4*.
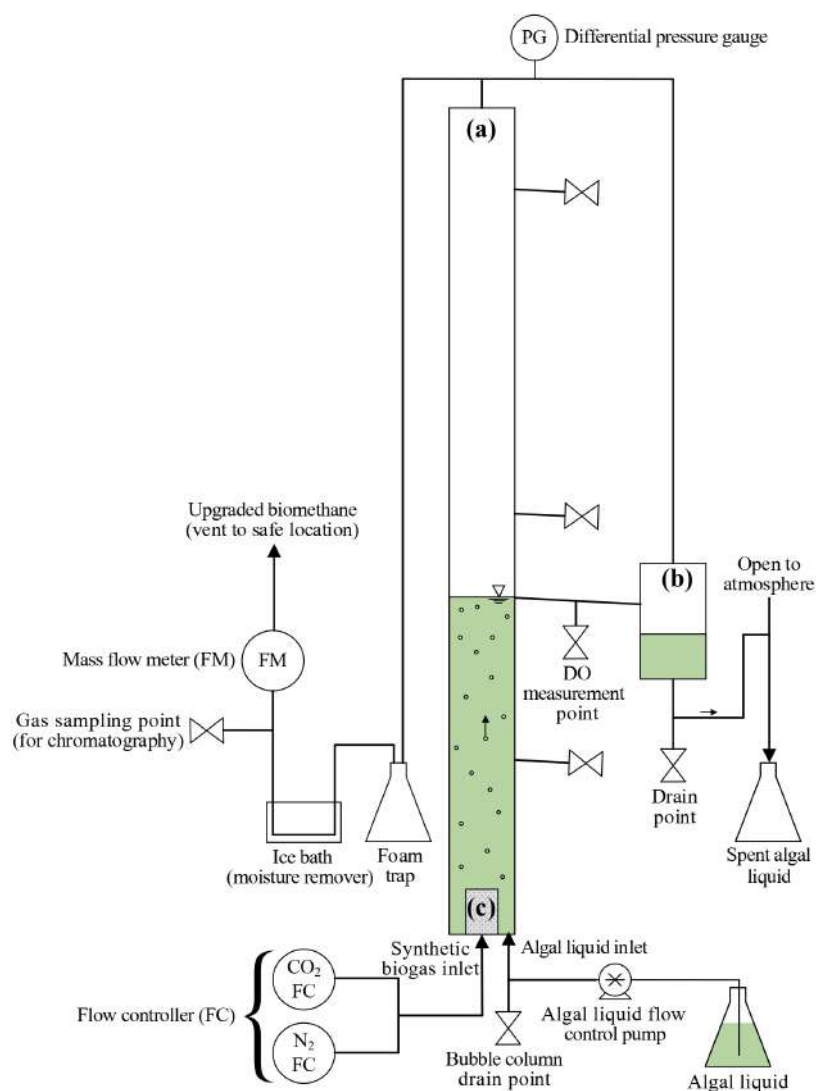

Fig. 2. Diagrammatic representation (not to scale) of the experimental setup for the screening design of experiments where **(a)** is the primary bubble column, **(b)** is the gas-liquid separator, and **(c)** is the gas diffuser.

2.3. Experimental design

2.3.1. Screening design of experiments

The Taguchi OA as a screening design of experiments was used to quantitatively determine the most critical design factors and their corresponding settings at which both the desired output is achieved, and the system resilience is maximised (Krishnaiah and Shahabudeen, 2012; Montgomery, 2012). This method was selected as it provides a robust, balanced, and unbiased technique to compare the main effects of the design factors independently of each other with a minimum number of experiments (Krishnaiah and Shahabudeen, 2012; Chiranjeevi and Mohan, 2016; Awty-carroll et al., 2020). Additionally, a few interactions among the design factors can also be studied (Rao et al., 2008; Krishnaiah and Shahabudeen, 2012). In this concept, each design factor is studied at two levels ("high" or "low" for quantitative factors or "on" or "off" for qualitative ones) to systematically record and rank their influences on the desired outcome (Smith et al., 2016). **Figure 3** outlines the step-by-step methodology of the Taguchi experimental design used in the present study. A brief description of each step has been provided in the following sections, further details of which can be found in multiple pieces of literature and textbooks (Roy, 2010; Krishnaiah and Shahabudeen, 2012).

2.3.2. Selection of process responses as bubble column performance criteria

To prevent confounding and to develop a perspective on the bubble column design, cost, and operations, system performance was assessed in terms of CO_2 removal and oxygen stripping from the microalgal medium into the biomethane. CO_2 removal efficiency (R_{eff, CO_2}) (%); the mean steady-state absorption rate of CO_2 (R_{abs,CO_2}) (mol/L/s); and the mean overall CO_2 mass transfer coefficient $k_{G_{CO_2}}a$ (h^{-1}) were used to assess CO_2 removal (Chen et al., 2015). To measure oxygen stripping, the oxygen concentration in the upgraded biomethane ($O_{2,\%,BM}$) (%), together with the flow rate of oxygen in the outlet biomethane ($O_{2,BM}$) (mL_n/min) were studied.

Assuming a closed system with no loss of gases, R_{eff, CO_2} was calculated from the inlet molar flow rate of CO_2 in the biogas ($N_{CO_2,BG}$) and the outlet molar flowrate of CO_2 in the biomethane ($N_{CO_2,BM}$) (mol/min) according to **Equation 3**. The corresponding mean steady-state absorption rate of CO_2 (R_{abs,CO_2}) (mol/L/s) is described in **Equation 4** in which V_{BC} denotes the liquid volume in the bubble column (L) (Chen et al., 2015). The following assumptions were made: i) a two-phase system with minimal influence of the solid phase (Clark, 1990; Deckwer et al., 1980); ii) a thoroughly mixed homogeneous system that can be considered as a plug flow and can be well represented by the two-film theory (Fernández et al., 2017; Chen and Lin, 2018); iii) isothermal conditions conforming to the ideal gas laws; and iv) fast chemical reactions occurring above pH 8 (Borhani et al., 2015). Finally, the mean overall mass transfer coefficient for CO_2 absorption $k_{G_{CO_2}}a$ (h^{-1}) was estimated after Chen and Lin (2018) *via* **Equation 5**, where G represents the total gas flow rate in the influent biogas in mL_n/s.

$$R_{eff, CO_2} = \frac{N_{CO_2,BG} - N_{CO_2,BM}}{N_{CO_2,BG}} \times 100 \qquad \text{Eq. 3}$$

$$R_{abs,CO_2} = \frac{N_{CO_2,BG} - N_{CO_2,BM}}{V_{BC}} \qquad \text{Eq. 4}$$

$$k_{G_{CO_2}}a = \frac{G}{V_{BC}} \cdot \ln \frac{N_{CO_2,BG}}{N_{CO_2,BM}} \qquad \text{Eq. 5}$$

2.3.3. Selection of design factors and their levels

Seven controllable variables or design factors affecting the operation of the bubble column in photosynthetic biogas upgrading were selected for comparative assessment, namely: superficial gas velocity (u_c); the liquid to gas flow rate (L/G) ratio; EBRT; liquid inlet pH; liquid inlet alkalinity (Alk); temperature (T_{col}); and algal concentration in the liquid circulating in the bubble column (C_{alg}). As discussed in *Section 1.2*, and compiled in **Table 1**, all factors except algal concentration and EBRT have been
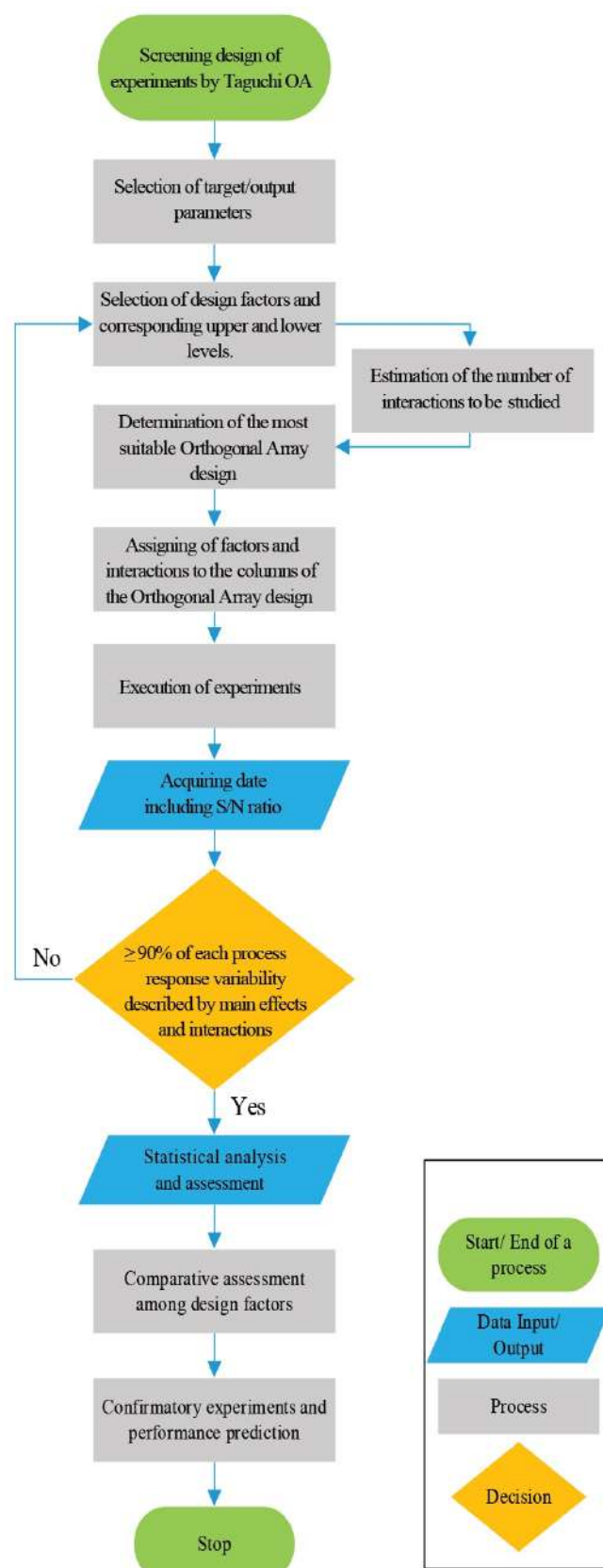

Fig. 3. Outline of the Taguchi screening design of experiments using orthogonal arrays.

separately investigated for their importance to the operations of the overall photosynthetic biogas upgrading system. While factors such as the pH and alkalinity would need to be optimised, understanding the relative importance of superficial gas velocity is important in order to increase the throughput of the bubble column. On the contrary, the influence of EBRT and algal concentration have only been evaluated explicitly by Bahr et al. (2014) and del Rosario Rodero et al. (2020b), respectively. However, in a previous work by the authors (Bose et al., 2019), these factors were discussed to be of potentially considerable importance and hence are selected for assessment herein. Indeed, decreasing the EBRT to current industrial levels is critical towards ensuring the use of state-of-the-art bubble columns for photosynthetic biogas upgrading, as this would reduce construction and operation costs. Other variables, such as the CO_2 and H_2S content in biogas and the dissolved oxygen (DO) in the circulating algal liquid, which affect the bubble column operation, are exogenous to the bubble column design and hence not included in the design factors.

The upper and lower bound value of each design factor was selected by assessing current trends and future targets from literature as indicated in **Table 2**. However, for u_G and EBRT, the upper values were selected based on the limitation of the experimental setup described in *Section 2.2*. Thus, the maximum u_G and EBRT were limited to 0.2 cm/s and 15 min, respectively, although their maximum limits lie at 4 cm/s and 90 min, respectively. Additionally, the maximum algal density was fixed at 0.75 g-DW/L, limited by foaming of the algae medium observed during pre-experiments (Bose et al., 2021). However, it is still representative of the algal concentrations obtained in closed and open photobioreactors (Hu et al., 1996; Costa et al., 2003). Similarly, the lower and upper temperature values correspond to the tolerable and ideal values for *S. platensis* (De Oliveira et al., 1999).

2.3.4. Selection of Taguchi OA, interactions, and experimental trials

The Taguchi OA comprising 16 experimental trials (L_{16}) was selected to quantitatively compare (screen) seven factors (tested at two levels, referred to as "2^7"). Each design factor was assigned one column in the fifteen column L_{16} OA. The remaining eight columns were used to study two-factor interactions, namely: i) L/G vs pH; ii) L/G *vs.* u_G; iii) u_G *vs.* EBRT; iv) u_G *vs.* pH; v) u_G *vs.* Alk; vi) u_G *vs.* T_{col}; vii) pH *vs.* Alk; and viii) T_{col} *vs.* C_{alg}.

Table 2.
Design factors and corresponding levels.

Factor	Design factors	Notation	Level	
			Low (1)	High (2)
A	L/G Ratio	L/G	0.2	1
B	Superficial gas velocity (cm/s)	u_G	0.06	0.2
C	Empty bed residence time (min)	EBRT	6	15
D	Inlet pH	pH	9	10.5
E	Inlet alkalinity (g-IC/L)	Alk	1	2.5
F	Temperature (°C)	T_{col}	20	35
G	Algae concentration (g-DW/L)	C_{alg}	0.05	0.75

Accordingly, the following Taguchi OA structure was generated as shown in **Table 3**. All higher order interactions were neglected with fair confidence (Montgomery, 2012).

Experiments were conducted using each row in the selected L_{16} OA (**Table 3**) as individual experimental runs. Columns 1, 5, 6, 8, 10, 11, and 12 represent the different settings of the design factors for the 16 experimental runs; the remaining columns accommodated the interactions. Each run was triplicated and randomised to minimise repeatable errors, also referred to as systematic bias (Mehta, 2001), and to enable accurate estimation of the variations in the bubble column performance due to uncontrollable factors or noise.

2.3.5. Signal to noise (S/N) ratio

Each process response can be categorised as *i)* the signal or the intended response from the influence of the design factors and *ii)* unintended outcomes resulting from noise (Kishore et al., 2018). In the Taguchi method, to estimate the sensitivity of the main effects and interactions against the noise, the signal to noise (S/N) ratio is used as a qualitative metric (Roy, 2010). A higher value of the S/N ratio is always desired as,

Table 3.
L_{16} Taguchi Orthogonal array for screening design of 16 experiments (L_{16}) with seven factors (A-G) at two levels (2^7).

Run No.	Taguchi L_{16} columns														
	1	2	3	4	5	6	7	8	9	10	11	12	13	14	15
	L/G (A)	Interaction			u_G (cm/s) (B)	EBRT (min) (C)	Interaction	pH (D)	Interaction	Alk (g-IC/L) (E)	T_{col} (°C) (F)	C_{alg} (g/DW/L) (G)	Interaction		
1	0.2				0.06	6		9		1	20	0.05			
2	0.2				0.06	6		10.5		2.5	35	0.75			
3	0.2				0.2	15		9		1	20	0.75			
4	0.2				0.2	15		10.5		2.5	35	0.05			
5	0.2				0.06	15		9		2.5	35	0.05			
6	0.2				0.06	15		10.5		1	20	0.75			
7	0.2	pH *vs.* Alk	u_G *vs.* EBRT	L/G *vs.* u_G	0.2	6	T_{col} *vs.* C_{alg}	9	L/G *vs.* pH	2.5	35	0.75	u_G *vs.* pH	u_G *vs.* T_{col}	u_G *vs.* Alk
8	0.2				0.2	6		10.5		1	20	0.05			
9	1				0.2	6		9		1	35	0.05			
10	1				0.2	6		10.5		2.5	20	0.75			
11	1				0.06	15		9		1	35	0.75			
12	1				0.06	15		10.5		2.5	20	0.05			
13	1				0.2	15		9		2.5	20	0.05			
14	1				0.2	15		10.5		1	35	0.75			
15	1				0.06	6		9		2.5	20	0.75			
16	1				0.06	6		10.5		1	35	0.05			

the higher the value of S/N ratio, the more stable the process response is against the noise (Roy, 2010; Priyadarshi and Paul, 2019). Based on the objective, a process response might require to be minimised or maximised. When a process response needs to be maximised (R_{eff, CO_2}, R_{abs, CO_2}, $k_{G_{CO_2}}a$), the S/N ratio is classified as the larger-the-better (LB) criterion, given by **Equation 6**. On the contrary, when the process response is intended to be minimised ($O_{2,BM}$, $O_{2,\%,BM}$), the smaller-the-better (SB) S/N ratio is used, represented by **Equation 7** (Davis and John, 2018).

$$\left(S/N\right)_{LB} = -10\log_{10}\left[\frac{1}{n}\sum_i^n \frac{1}{y_{ij}^2}\right] \qquad \text{Eq. 6}$$

$$\left(S/N\right)_{SB} = -10\log_{10}\left[\frac{1}{n}\sum_i^n y_{ij}^2\right] \qquad \text{Eq. 7}$$

where y_{ij} refers to the ith output signal (i = 1,2,3) of the process response j (e.g., R_{eff, CO_2}) among n replicates (n = 3).

2.3.6. Determining the adequacy of the experimental design

Prior to analyses of results, a statistical test was performed to check the adequacy of the chosen experimental design. A general linear model *via* analysis of variance (ANOVA) (summarised in *Section 2.3.8*) was fitted, considering each replicate as a separate experiment (Myers et al., 2017). If the experimental design is adequate, the fitted model should be able to describe the majority of the variabilities in the process responses using the fifteen factors (seven main effects and eight interactions) chosen in the experimental design.

2.3.7. Interpretation of the experimental results

Based on the results of the Taguchi OA, the influence of the design factors on the performance of CO_2 removal and oxygen stripping in the bubble column were compared using the following steps:

Step 1: A main effects plot showing the mean process response at each level (low (1) or high (2)) of the design factors was first plotted to graphically identify the influence of the design factors on the mean process responses. This also allowed the identification of the design factor settings to obtain the desired process responses. The slope of the plot additionally indicates the influence of each design factor on the response (Antony, 2014); a positive slope shows an increase in response on increasing the design factor value and *vice-versa*.

Step 2: A similar main effects plot with the S/N ratio of the process response was then plotted. The design factor that caused the highest variation in the S/N ratio of the process response between its low and high setting was concluded to have the largest influence on the studied process response (Antony, 2014). All other design factors were then ranked subsequently.

Step 3: A general linear model *via* the ANOVA was then fitted to the S/N ratios to obtain the percentage contributions of the design factors and the interactions towards the process response (described in *Section 2.3.8*).

Step 4: A half normal probability plot was plotted to graphically compare the relative contribution of both the main effects of the design factors and the studied interactions on the process response (Ganapathy et al., 2009).

Step 5: A confirmatory pooled ANOVA was performed using only the design factors and interactions having over 95% contribution towards the process response to determine the factors (main effects and interactions) that are statistically significant (P < 0.05). All other factors were pooled under the error term. The higher value of 95% was selected to minimise the possibility of falsely rejecting important design factors, also known as type II error in statistical jargon (Montgomery, 2012; Jones, 2016). Especially for screening experiments, such a false rejection effecting the omission of a major design factor from future detailed designs could severely limit the development of a product or process (Jones, 2016).

2.3.8. Analysis of variance (ANOVA)

ANOVA provides a statistical approach to quantify the variations in the process responses resulting from the main effects and interactions (Kishore et al., 2018). Additionally, it also provides an estimation of the unexplained

variations or errors resulting from noise, experimental limitations, and assumptions (Kishore et al., 2018). The results of the multivariate ANOVA are typically represented as a table having the following entries (not in order): *i)* sources, signifying the design factors, interactions, errors, and the cumulative total of variations *ii)* degree of freedom (DoF); *iii)* adjusted sum of squares (Adj SS); *iv)* adjusted mean squares (Adj MS); *v)* the Fischer's F distribution (F-value); *v)* P-value; and *vii)* contribution (%$_{contrib}$) of each main effect, interaction, and error term towards the process response calculated by **Equation 8**.

$$\%_{contrib} = \frac{AdJ\,MS_{source}}{AdJ\,MS_{total}} \times 100 \qquad \text{Eq. 8}$$

In the ANOVA table, the degrees of freedom of a source or a model signifies the number of independent inputs required to describe itself (Montgomery, 2012). The F-value signifies the extent to which the variance due to a certain source compares with variance arising from the errors, i.e., how large or small the variations due to a certain source is with respect to the unexplained variations (Mohsin et al., 2020). Irrespective of its value, to evaluate if the F value as obtained is true, the corresponding P-value is calculated as the probability of the F value being obtained by random chance (Montgomery, 2012; Mohsin et al., 2020). Thus, a higher P-value indicates a greater probability of obtaining the F-value as a random chance and hence, a lower statistical significance of the calculated F-value. Contrarily, a lower P-value indicates a lesser probability of obtaining the F-value as a chance and thus, indicates a greater statistical significance of the calculated F-value. Additionally, for each general linear model, a model-F value is also generated by ANOVA that signifies the predictability of the model in comparison with a model that contains no independent variables. The model F-value must be higher than the value of the F statistic below which there exists a probability of α to mistakenly reject a true null hypothesis (i.e., the two variances are equal) (Kim, 2017), also known as the critical F-value (F_{crit}). F_{crit}, given in the form of $F_{\alpha(k-1, n_{ex}-k)}$ can be obtained from standard statistical handbooks, where k is the number of predictors in the model and n_{ex} is the total number of experimental trials. The respective model P value signifies the probability that the model F-value was derived from the influence of noise, and hence, a lower P-value is always desired (Kishore et al., 2018; Mohsin et al., 2020). The details of each of these statistics can be further explored in multiple pieces of literature and textbooks (Roy, 2010; Montgomery, 2012).

2.3.9. Performance prediction and confirmatory experiment

Using the statistically significant (P < 0.05) main effects and interactions, the biomethane composition exiting the bubble column under different conditions was predicted by a general linear equation in the form expressed in **Equation 9**.

$$\hat{Z} = A_0 + A_i X_i + A_{ij} X_i X_j \qquad \text{Eq.9}$$

where A_0 represents the constant of the model, A_i is the coefficient of each design factor X_i, and A_{ij} is the coefficient of each interaction between the design factors X_i and X_j. These coefficients are derived from the ANOVA analysis and also signify the relative quantitative influence of main effect and interaction on the process response variable (Smith et al., 2016). CO_2 removal efficiency (R_{eff, CO_2}) (%) and O_2 outflow rate ($O_{2,BM}$) (mL$_n$/min) were used as estimates for CO_2 and O_2 flow rates, respectively, from which their respective compositions in biomethane can then be derived. The goodness of fit of the model was assessed with regards to the regression coefficient R^2 (a measure of the agreement between predicted and actual values) and standard error of regression (S), signifying the average deviation of the observed data from the predicted model.

As the predictive regression equations were derived from ANOVA that utilises the S/N ratio statistic, **Equations 10** and **11** were used to convert the predictors back into actual responses for physical interpretation.

$$\hat{R}_{eff, CO_2} \cong \left[10^{\left(-(S/N)_{R_{eff, CO_2}}/10\right)}\right]^{-0.5} \qquad \text{Eq. 10}$$

$$\hat{O}_{2,\text{BM}} \cong \left[10^{(-(S/N)_{O_2,BM}/10)}\right]^{0.5} \qquad \text{Eq. 11}$$

where $\hat{R}_{\text{eff, CO}_2}$ and $\hat{O}_{2,\text{BM}}$ predicts for $R_{\text{eff, CO}_2}$ and $O_{2,\text{BM}}$, respectively. For each prediction, the 95% confidence interval ($CI_{95\%}$) was calculated by **Equation 12** (Roy, 2010)

$$CI_{95\%} = \hat{Z} \pm \sqrt{\frac{F_{0.05}(f_1,f_2) \times V_{error}}{n_{eq}}} \qquad \text{Eq. 12}$$

where $\hat{Z}$ ($\hat{R}_{\text{eff, CO}_2}$ and $\hat{O}_{2,\text{BM}}$) represents the predicted value and V_{error} stands for the variance in the error term. $F_{0.05}(f_1, f_2)$ is the F-value for DoF f_1 and f_2 at a significance level of 0.05 (confidence interval of 95%); where $f_1 = 1$, being the DoF of factors in the regression model and f_2 is the DoF of error term. This value of F is obtained from the F-tables from any standard statistical handbook. n_{eq}= Number of trials/$(f_1 + f_{factors})$ is known as the number of equivalent replications in which, $f_{factors}$ is the DoF of factors in the regression model, also equal to 1.

On the other hand, the 95% prediction interval ($PI_{95\%}$) for each prediction was calculated *via* **Equation 13** (Kitchin, 1994) to estimate the range within which 95% of the predicted values would lie with a confidence of 95%.

$$PI_{95\%} = \hat{Z} \pm t_{\alpha/2,(n-2)} \times \sqrt{\frac{SSE}{n-2}\left(1 + \frac{1}{n} + \frac{n(x^*-\bar{x})^2}{n\sum_{i=1}^{n}x_i - \left(\sum_{i=1}^{n}x_i\right)^2}\right)} \qquad \text{Eq. 13}$$

In the above equation, $t_{\alpha/2,(n-2)} = t_{0.05/2,(16-2)}$ is the $100(\alpha/2)$ percentile of the student's t-distribution with 14 degrees of freedom with the significance level (α) as 0.05 and n=16 from the 16 experimental runs. SSE denotes the sum of squared errors given as $\sum_{i=1}^{n}(x_i - \bar{x})^2$ where x_i is the value of the ith observation and $\bar{x}$ indicates the value of the mean of all observations. x^* represents the value of the independent predictor for predicting the corresponding $\hat{Z}$.

A confirmatory experiment was performed at a chosen level of control (different from the sixteen Taguchi trial settings) based on the experimental trials and conclusions from the screening design of experiments. The mean from the triplicated experiment (Z_{actual}) was compared with the predicted output ($\hat{Z}$) with the following consideration (**Eq. 14**):

$$\hat{Z} - CI_{95\%} \leq Z_{actual} \leq \hat{Z} + CI_{95\%} \qquad \text{Eq. 14}$$

Finally, using the predictive regression equations, the variation in biomethane composition was studied between the interval of pH 9 (factor level "1") and pH 10.5 (factor level "2") and L/G ratio 0.2 (factor level "1") and 1 (factor level "2"). For this, the superficial gas velocity was varied at two levels, namely 0.06cm/s (factor level "1") and 0.2 cm/s (factor level "2"). All other design factors were fixed to maximise the S/N ratio.

2.4. Data and analysis

2.4.1. Data acquisition

The steady state criteria to acquire measurements and assess the system performance were defined as follows: *i)* a constant gas flow rate (less than 5% variation on average), and *ii)* less than 5% variation in the pH of the liquid at the outlet of the gas liquid separator over a period of 120 s each. Gas was sampled for compositional assessment *via* chromatography from a tap placed between the ice bath and the mass flow meter, as indicated in **Figure 2**. A 10 mL plastic syringe was used for this purpose. The DO content of the outlet liquid was measured near the bubble column outlet to prevent distortion of results from the ingression of oxygen.

2.4.2. Analytical procedures

The algal density was measured as optical density at a wavelength of 530 nm in a VWR® V-3000 PC manual spectrophotometer calibrated to the microalgae dry weight. All pH and DO measurements were performed using a handheld pH meter (VWR® MD 8000H Multi Parameter Meter) fitted with respective interchangeable probes (pHenomenal VWR® pH/ORP sensor/ pHenomenal VWR® OPOX 11-3 sensor). Alkalinity was measured using Titronic® Universal Titrator as per Method No. 2320 B of APHA (American Public Health Association-APHA, 1992) by titrating up to pH 4.5. Algal solution for photosynthetic biogas upgrading was prepared by diluting 2-3 g-DW/L microalgae culture with distilled water to the algal concentration. In an actual photosynthetic biogas upgrading cycle, algae will be circulated after cultivation to ensure CO_2 uptake. As such, nutrient adjustment was not performed in order to resemble the nutrient replete medium after cultivation. The DO content in the inlet liquid varied between 6 to 10 mg/LO_2 as per those obtained during *S. platensis* cultivation and are representative of those typically obtained in photobioreactors (Yang et al., 2017).

Volumetric gas flow rate was measured in terms of equivalent N_2 flow using a thermal mass flow meter (Bronkhorst® F101D Low-ΔP-Flow Thermal Mass Meter). CO_2, N_2, and O_2 content in the gas were analysed by a gas chromatograph (GC; Agilent® 7890B, USA) equipped with a thermal conductivity detector and a 5A column. The online gas Converter tool by Fluidat® (Bronkhorst®) was used to convert the recorded gas flow to the volumetric flow in terms of its constituents based on the composition obtained from the gas chromatograph. The actual gas flow rate and composition were obtained after a further correction step to the individual oxygen and nitrogen flow rates. This was done because noticeable air (N_2 and O_2) ingress by diffusion into the gas tubing used in the experiment was recorded during pre-experiments (Bose et al., 2021). To obtain the correction terms needed to remove this interference from the recorded flowrates, N_2 was blown into the system at the same rate as that used in the subsequent experiments, and the gas composition and flow rates were measured. The additional O_2 and N_2 flow rates that were obtained as correction factors were subtracted from the respective biomethane component flow rates to calculate the final biomethane composition and flow rate.

2.5. Statistical analysis

All statistical analyses, including the design and assessment of the Taguchi L_{16} OA, were performed using Minitab® software version 19 (Minitab LLC., Pennsylvania, USA). For all assessments, a confidence level of 95% (P < 0.05) was selected for asserting statistical significance.

3. Results and Discussion

3.1. Validation of the bubble column operation

The biomethane composition generated during each trial, together with the pH of the liquid at the bubble column outlet and the process responses (e.g., $R_{\text{eff, CO}_2}$ and $R_{\text{abs,CO}_2}$) are compiled in **Table 4**. Out of all the trials, grid quality biomethane was obtained only in Run 4 (L/G ratio of 0.2, pH 10.5 and values for other 5 variables); the respective CO_2 and O_2 in the outlet biomethane was 0% ± 0.00% and 0.23% ± 0.1%.

A mass balance approach was used to validate the outcomes of O_2 and N_2 in the upgraded biomethane. Investigative assessments were performed on four experimental runs (Runs 5, 8, 9, and 12 of the Taguchi OA) that use low algal concentration. This was to ensure that the O_2 in the biomethane is derived primarily from stripping of the DO of the circulating algal liquid with minimal influence of the O_2 released by the active photosynthesising microalgae. Considering no O_2 in the inlet biogas, a good agreement was found between the theoretical and the experimental values for oxygen in the outlet biomethane (**Fig. 4a**). On the other hand, as shown in **Figure 4b**, the N_2 flow in the biogas generally matched closely with that in the biomethane, confirming the assumption of minimal N_2 stripping.

CO_2 removal performance was validated by comparing the values of the evaluation metrics with data from the literature. As can be seen from **Table 4**, the CO_2 removal efficiencies varied between 19.29% and 100%; the corresponding absorption rates ($R_{\text{abs,CO}_2}$) ranged from 0.036×10^{-4} mol/L/s to 0.459×10^{-4} mol/L/s. The volumetric mass transfer coefficient ($k_{G_{CO_2}}a$) varied from 0.87 h^{-1} (0.0002 s^{-1}) to 97.64 h^{-1} (0.027 s^{-1}). The results are in a close agreement with those reported by Chen et al. (2015), who studied the behaviour of CO_2 removal with NaOH.
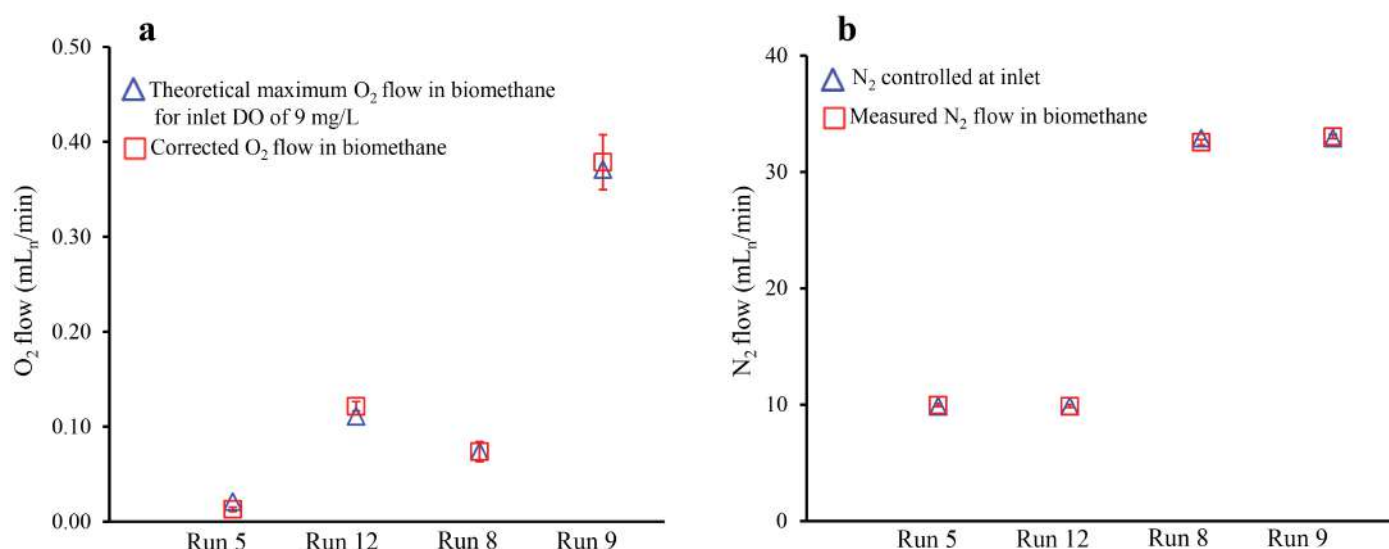
Fig. 4. Comparison between expected and measured values of **(a)** O_2 and **(b)** N_2 to validate the bubble column operations and measurement techniques utilised.

Table 4.
Results from the 16 experimental runs in triplicates performed on the L_{16} Taguchi Orthogonal Array along with the S/N ratios of the responses selected for factors screening studies.

Biomethane composition		Liquid outlet pH	R_{eff,CO_2} (%)	R_{abs,CO_2} (mol/L/s)	$k_{G_{CO_2}}a$ (h^{-1})	$O_{2,BM}$ (mL$_n$/min)	S/N ratios				
CO$_2$ (%)	O$_2$ (%)						R_{eff,CO_2} $^\zeta$	R_{abs,CO_2} $^\zeta$	$k_{G_{CO_2}}a$ $^\zeta$	$O_{2,\%,BM}$ §	$O_{2,BM}$ §
27.76 ± 0.07	0.16 ± 0.06	7.74 ± 0.04	40.44 ± 0.46	0.189 ± 0.002	5.23 ± 0.08	0.023 ± 0.008	-7.87	14.37	-14.48	55.32	32.33
6.47 ± 1.09	0.28 ± 0.13	9.68 ± 0.02	89.48 ± 1.87	0.418 ± 0.009	22.91 ± 1.83	0.030 ± 0.014	-0.97	27.12	-7.59	50.07	29.55
34.23 ± 1.71	0.51 ± 0.12	8.26 ± 0.01	19.29 ± 3.61	0.036 ± 0.007	0.87 ± 0.18	0.263 ± 0.062	-14.79	-1.83	-29.38	45.66	11.36
0.00 ± 0.00*	**0.23 ± 0.01***	**9.49 ± 0.07**	**100.00 ± 0.00**	**0.187 ± 0.000**	**40.38 ± 0.00**	**0.078 ± 0.004**	**0.00**	**32.12**	**-14.58**	**52.56**	**22.16**
23.99 ± 0.47	0.09 ± 0.02	8.19 ± 0.07	52.11 ± 0.85	0.097 ± 0.002	9.92 ± 0.24	0.013 ± 0.002	-5.66	19.92	-20.24	60.01	37.63
7.69 ± 0.42	1.28 ± 0.24	9.18 ± 0.06	87.35 ± 0.74	0.163 ± 0.001	27.87 ± 0.78	0.139 ± 0.027	-1.18	28.89	-15.75	37.71	17.011
32.06 ± 0.09	0.39 ± 0.02	7.82 ± 0.07	29.57 ± 0.68	0.138 ± 0.003	1.06 ± 0.03	0.187 ± 0.013	-10.59	0.51	-17.21	48.21	14.55
13.21 ± 0.89	0.19 ± 0.03	7.94 ± 0.04	77.01 ± 1.66	0.359 ± 0.008	4.46 ± 0.22	0.074 ±0.011	-2.28	12.96	-8.89	54.18	22.56
18.34 ± 0.93	0.94 ± 0.06	7.97 ± 0.04	66.25 ± 1.69	0.309 ± 0.008	3.29 ± 0.15	0.379 ± .029	-3.58	10.33	-10.20	40.54	8.41
1.06 ± 0.52	1.39 ± 0.04	10.15 ± 0.02	98.35 ± 0.84	0.459 ± 0.004	12.79 ± 1.42	0.471 ± 0.019	-0.14	21.96	-6.76	37.12	6.53
14.23 ± 0.55	0.82 ± 0.10	8.15 ± 0.02	75.07 ± 0.5	0.140 ± 0.001	18.71 ± 0.27	0.094 ± 0.011	-2.49	25.44	-17.07	41.70	20.48
0.33 ± 0.47	1.21 ± 0.04	10.09 ± 0.06	99.48 ± 0.73	0.186 ± 0.001	97.64 ± 29.35	0.121 ± 0.005	-0.04	38.14	-14.62	38.34	18.30
2.52 ± 0.18	0.88 ± 0.18	8.39 ± 0.04	96.06 ± 0.27	0.179 ± 0.001	13.07 ± 0.29	0.300 ± 0.066	-0.35	22.32	-14.93	40.96	10.29
0.00 ± 0.00	1.35 ± 0.2	9.84 ± 0.04	100.00 ± 0.00	0.187 ± 0.000	40.38 ± 0.00	0.450 ± 0.065	0.00	32.12	-14.58	37.28	6.85
10.13 ± 0.67	0.73 ± 0.25	8.54 ± 0.07	82.60 ± 1.42	0.386 ± 0.007	17.69 ± 0.85	0.082 ± 0.026	-1.66	24.93	-8.28	42.24	21.28
3.13 ± 1.04	0.89 ± 0.14	10.06 ± 0.05	95.10 ± 1.46	0.444 ± 0.007	31.01 ± 3.51	0.094 ± 0.019	-0.44	29.68	-7.06	40.94	20.39

*: Denotes grid quality biomethane was achieved; ζ: Denotes process responses using larger-the-better (LB) criteria; §: Denotes process responses using smaller-the-better (SB) criteria.

Operating between pH of 10 and 11, temperatures of 25 °C and 35 °C and L/G ratios of 0.05 and 0.16 , $k_{G_{CO_2}}a$ extended from 54 h^{-1} to 154.8 h^{-1}, while the lowest and the highest absorption rates were 1.03×10^{-4} mol/L/s and 2.13×10^{-4} mol/L/s, respectively; the higher values recorded at higher pH and temperature. It must be mentioned here that as the CO_2 absorption reaction is primarily driven by carbonate-derived [OH]$^-$ ions (Hikita et al., 1976; Knuutila et al., 2010), the comparison with NaOH is reasonable. These comparisons were concluded as sufficient to validate the bubble column operations and measurement techniques for acceptable prediction of the experimental outcomes.

3.2. Adequacy of the experimental design

The result of the design adequacy test as explained in *Section 2.3.6* is summarised in **Table 5**. For each process response, the chosen 15 factors (seven main effects and eight interactions) were able to account for at least over 90% of the variations in each process response. CO_2 removal efficiency and absorption rates were almost sufficiently described, with an unknown variation of less than 0.5% in the outcome. However, to describe the hydrodynamic aspect of CO_2 absorption, a few other variables might be

Table 5.
Results of ANOVA for each process response considering each replicate as a separate experimental trial as an adequacy test of the designed screening experiment.

Regression parameters	R_{eff,CO_2} (%)	R_{abs,CO_2} ($\times 10^{-4}$ mol/L/s)	$k_{G_{CO_2}}a$ (h^{-1})	$O_{2,BM}$ (%)	$O_{2,BM}$ (mL$_n$/min)
Total DoF	47	47	47	47	47
Model DoF	15	15	15	15	15
Error DoF	32	32	32	32	32
Explained variations (Model contribution) (%)	99.72	99.86	90.78	92.09	95.76
Unexplained variations (%)	0.28	0.14	9.22	7.91	4.24
Model F value	762.26 (P < 0.001)	1520.37 (P < 0.001)	21.01 (P < 0.001)	25.02 (P < 0.001)	48.22 (P < 0.001)
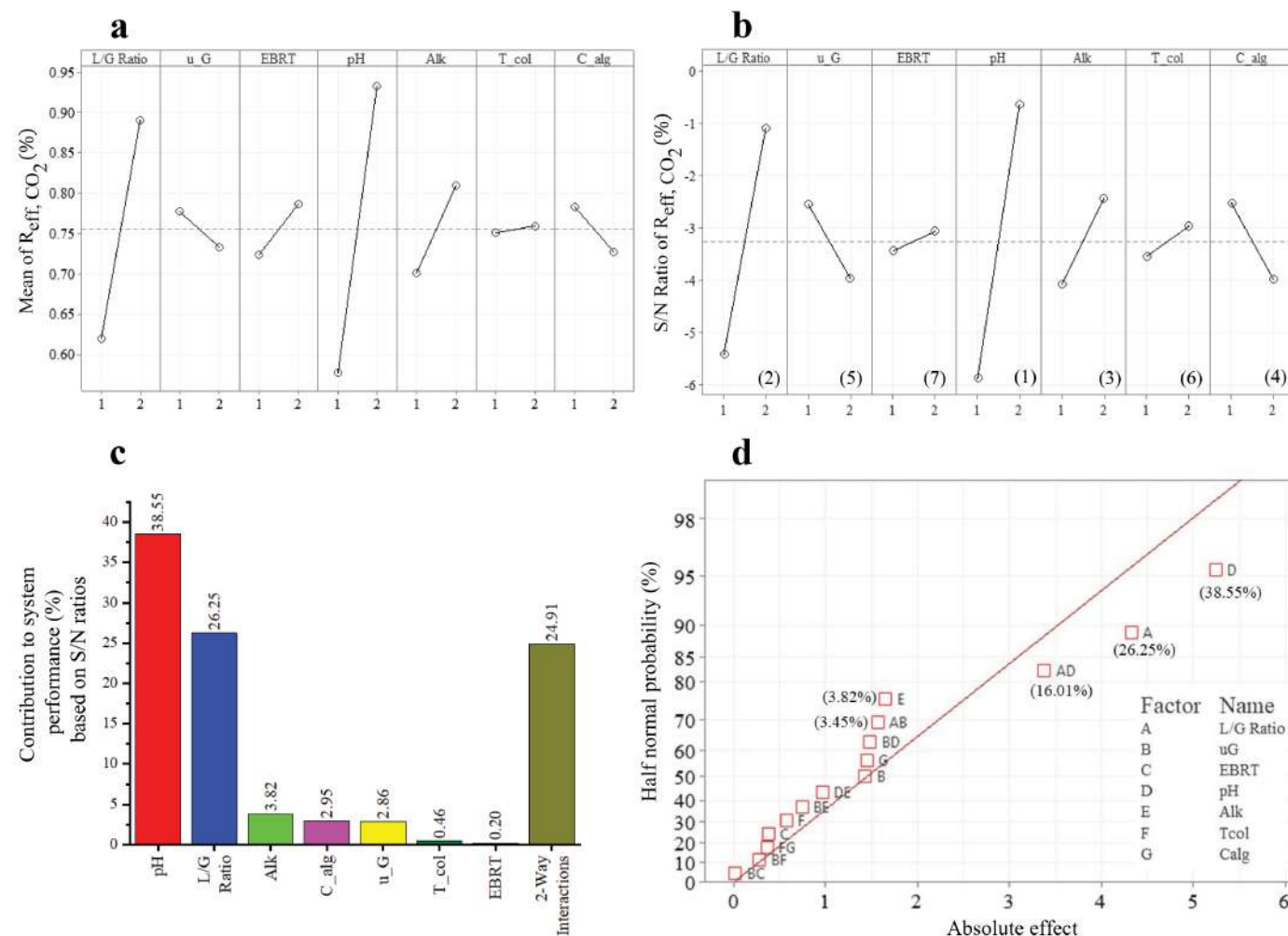
Fig. 5. Analysis plots for relative influence of design factors on CO_2 removal efficiency: **(a)** Main effects plot with mean; **(b)** Main effects plots with S/N ratio. The rank of each design factor is included in parentheses; **(c)** Contribution of each design factor and interactions on the overall system outcome; and **(d)** Half normal probability plot with the relative contribution of major effects highlighted in brackets.

required to explain the remaining 9.22% of the system fluctuations. The chosen screening design was able to explain over 92% of the variations for O_2 stripping during biogas upgrading.

From a statistical perspective, the F values of the fit models were also much higher than the critical F-value ($F_{0.05(15,32)}$) (k = 16 including the constant and N = 48 from 16 triplicated experiments) of 1.99 at a 95% confidence level with a corresponding P value less than 0.001. This indicates the statistical significance of the selected main effects and interactions to describe the bubble column performance in photosynthetic biogas upgrading (Shah et al., 2013).

3.3. Results of the screening design of experiments

The following section summarises the results from the Taguchi OA for each process response describing CO_2 removal and O_2 stripping in the bubble column.

3.3.1. CO_2 removal efficiency (R_{eff, CO_2})

Figure 5a shows the main effects plot with mean CO_2 removal efficiency (R_{eff, CO_2}). The highest variation in the mean response was

obtained from the variation of pH, closely followed by that due to the L/G ratio. For both these factors, a higher setting increases the mean response, i.e., improves the CO_2 removal efficiency. Higher alkalinity and empty bed residence time were also found to increase the CO_2 removal efficiency signifying a lower average CO_2 content in the upgraded biomethane. Between 20 °C (factor level "1") and 35 °C (factor level "2"), temperature caused a negligible increase in R_{eff, CO_2}, closely resembling the results presented by Chen et al. (2015). On the other hand, an increase in superficial gas velocity and algal concentration decreased the CO_2 removal efficiency.

A study of the main effects plot of the S/N ratio in **Figure 5b** also reveals a similar trend for the design factors. Operations at a higher pH, L/G ratio, alkalinity, and temperature setting would result in more robust operations (higher S/N ratios). The effect of EBRT on the system fluctuations was minimal (minimal variation in the S/N ratio). An increased superficial gas velocity and algal concentration would cause larger system variabilities (lower S/N ratios and negative slope of the main effects plot). Comparing variation of the S/N ratio corresponding to each main effect (**Fig. 5b**), pH was found to be the most influential factor towards the efficiency of CO_2 removal from biogas followed by L/G ratio and alkalinity. These are followed by microalgae concentration and superficial gas velocity, however, as explained before, in a negative way. Temperature and EBRT were obtained as the two of the least affecting factors in the selected experimental regime to affect the removal efficiency of CO_2.

The quantification of the rankings and influences provided in **Figure 5c** shows the contribution of the different main effects and the two-way interactions (pooled together) towards the process response (CO_2 removal efficiency). Matching the observations from the main effects plots, pH was found to account for 38.55% of the variations in the CO_2 removal efficiencies followed by L/G ratio (26.25%) and alkalinity (3.82%). Interactions were found to play a major role, whereby they were responsible for almost 25% of the system variations. To obtain a further detailing of the results, a half normal probability plot (**Fig. 5d**) was used to demonstrate the influence of the fifteen factors (seven main effects and eight interactions). In it, the factors that have the highest influence on the process response and are also statistically significant ($P < 0.05$) usually lie further away from linearity, indicated by the straight line with a 45° slope (Ganapathy et al., 2009; Myers et al., 2017). As expected, pH and L/G ratio can be seen to be located furthest away from the 45° linearity. Moreover, it can be clearly interpreted that of all the interactions, the interaction between pH and L/G ratio had the highest influence (above 16%) on the efficiency of CO_2 removal. Alkalinity and the interactions of superficial gas velocity with pH and L/G ratio could also be seen to deviate somewhat from linearity, indicating their possible influence on the process response. All other factors being nearer to the 45° line could be concluded to have a minimal influence on the efficiency of CO_2 removal from biogas.

Table 6.
Results of ANOVA assessment for CO_2 removal efficiency with main effects and interaction contributing over 95% towards the output response.

Source	DoF	Adj SS	Adj MS	F-Value	P-Value	Contribution (%)
pH[*]	1	110.024	110.024	88.92	<0.001	38.55
L/G[*]	1	74.911	74.911	60.54	<0.001	26.25
L/G *vs.* pH[*]	1	45.692	45.692	36.93	0.001	16.01
Alk[*]	1	10.893	10.893	8.8	0.021	3.82
L/G *vs.* u_G[*]	1	9.842	9.842	7.95	0.026	3.45
u_G *vs.* pH[*]	1	8.773	8.773	7.09	0.032	3.07
C_{alg}[*]	1	8.425	8.425	6.81	0.035	2.95
u_G[*]	1	8.159	8.159	6.59	0.037	2.86
Pooled error	7	8.661	1.237	-	-	3.03
Cumulative total	15	285.38	-	-	-	-

[*]Denotes the statistically significant ($P < 0.05$) source (factors).

To confirm the above hypothesis, a pooled ANOVA was performed; the results are indicated in **Table 6**. As can be seen, all the main effects of pH, L/G ratio, alkalinity, superficial gas velocity, and algal concentration were found to be statistically significant ($P < 0.05$). The statistically significant interactions to affect CO_2 removal efficiency were those between pH and L/G ratio and between superficial gas velocity and pH and L/G ratio.
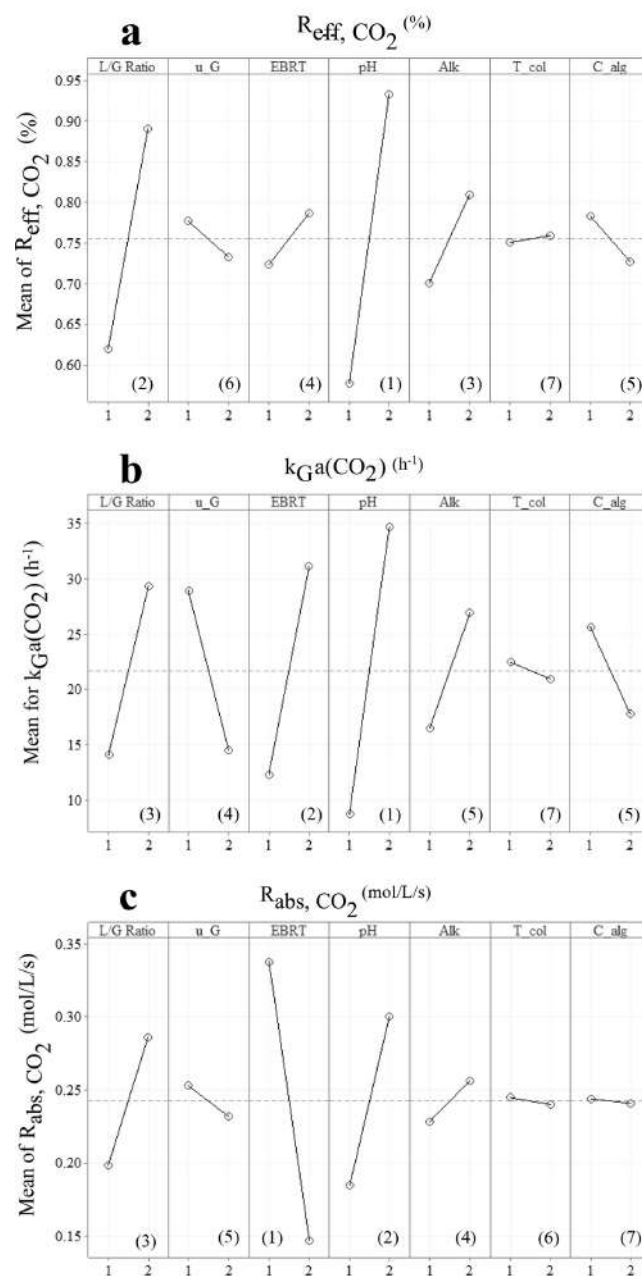
Fig. 6. Interactive effects between **(a)** pH and L/G ratio; **(b)** superficial gas velocity (u_G) and pH; and **(c)** superficial gas velocity (u_G) and L/G ratio on CO_2 removal efficiency.

Figure 6 shows the statistically significant ($P < 0.05$) interactions affecting CO_2 removal efficiency. For the interactive effect between L/G ratio and pH, depicted in **Figure 6a**, at lower pH levels (pH 9, factor level of "1"), L/G ratio can be seen to have a greater influence on the performance of the CO_2 removal efficiency (higher variation in the S/N ratio).
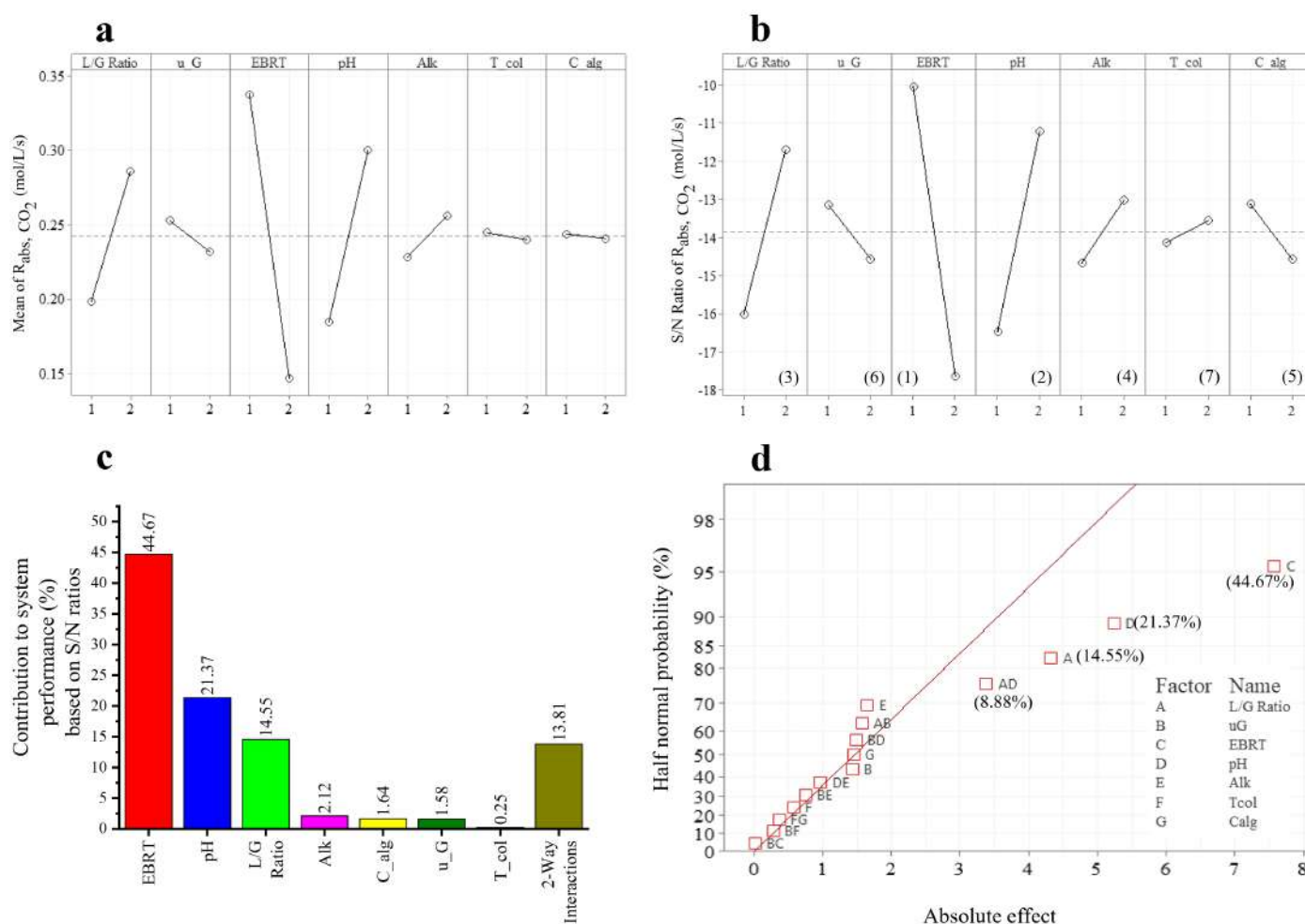
Fig. 7. Analysis plots for relative influence of design factors on mean steady state rate of CO_2 absorption: **(a)** Main effects plot with means; **(b)** Main effects plots with S/N ratio. The rank of each design factor is included in parenthesis; **(c)** Contribution of each design factor and interactions on the overall system outcome; and **(d)** Half normal probability plot with the relative contribution of major effects highlighted in brackets.

Accordingly, to reduce the operating pH, the L/G ratio must be increased to ensure effective CO_2 removal performance, i.e., ensure a higher S/N ratio. However, under high pH levels (pH 10.5, factor level of "2"), much more flexibility in operation with regards to L/G ratio can be envisaged. Indeed, as can be seen from **Figure 6a**, even at a low L/G of 0.2 ratio (factor level "1"), a pH of 10.5 (factor level "2") would ensure a high CO_2 removal efficiency indicated by higher system robustness or S/N ratio. The subsequent increase in the system performance on increasing the L/G ratio to 1 (factor level "2") would hence be minimal.

Respectively, **Figures 6b** and **c** reveal that both a high pH and a high L/G ratio would allow the superficial gas velocity and hence the gas flow rate to be increased without a substantial drop in CO_2 removal efficiency and hence the robustness of the bubble column operations. Of course, this is assuming the fact that all other effects not included in the interaction are set at the desirable set points that will maximise the S/N ratio (for example, alkalinity at 2.5 g-IC/L and algal concentration at 0.05 g-DW/L). In comparison, at lower pH and L/G ratios, the superficial gas velocity would cause larger fluctuations in the S/N ratio, lowering the CO_2 removal efficiency to the extent that grid quality biomethane might no longer be obtained.

3.3.2. Mean steady state CO_2 absorption rate (R_{abs,CO_2})

Similar to the discussion above, for the mean steady state CO_2 absorption rate (R_{abs,CO_2}), **Figures 7a-d** lead to the conclusion that EBRT is the most influential design factor. To understand this result, it must be understood that R_{abs,CO_2} signifies a lumped estimate of the kinetics of CO_2 absorption in the algal buffer solution. A large drop in the mean R_{abs,CO_2} at a higher EBRT, therefore, indicates a non-linear CO_2 absorption reaction along the length of the bubble column, with a rapid drop in the absorption rates along the height of the column. Correspondingly, the system also becomes more susceptible to uncontrollable variabilities, indicated by a drop in the S/N ratio (**Fig. 7b**). Nonetheless, for a specific bubble column with a fixed height of liquid column and hence a fixed EBRT, pH would have the largest positive influence followed by L/G ratio on R_{abs,CO_2}. Similar to CO_2 removal efficiencies, a higher setting of these design factors would thus yield both better performance (**Fig. 7a**, mean of response increases as the factor level increases) and more replicable responses (**Fig. 7b**, S/N ratio increases as factor level increases). **Figure 7c** confirms the ranking of factors showing their percentage contributions towards the process response. Additionally, the half normal probability plot in **Figure 7d** high-

lights the importance of the interaction between pH and L/G ratio on influencing the current process response.

The confirmatory ANOVA test in **Table 7** with factors affecting 95% of the variations in mean CO_2 absorption rate, revealed that EBRT, pH, and L/G ratio, and the interaction between pH and L/G ratio, were the only statistically significant ($P < 0.05$) factors. Thus, to optimise R_{abs,CO_2} in a specific bubble column (fixed EBRT), pH and L/G ratio would be sufficient to describe the system kinetics.

The only statistically significant ($P < 0.05$) interactive effect between pH and L/G ratio had a similar profile to that presented in **Figure 6a** for CO_2 removal efficiency (and hence not shown). Therefore, for a lower operating pH, to increase R_{abs,CO_2}, L/G ratio must be high. However, a higher pH would ensure a high R_{abs,CO_2} irrespective of the influence of the L/G ratio varying between 0.2 (factor level "1") and 1 (factor level "2").

### 3.3.3. Mean overall CO_2 mass transfer coefficient ($k_{G_{CO_2}}a$)

Following similar arguments as discussed above, it can be concluded from **Figures 8a-d** that pH had the highest influence on the mean overall CO_2 mass transfer coefficient, a measure of the hydrodynamic performance of the CO_2 absorption in the alkaline algal medium. This is followed (in order) by superficial gas velocity, L/G ratio, EBRT, and alkalinity, which all showed substantial influences on both the mean response and the S/N ratio. However, unlike the rest, an increase in the superficial gas velocity was found to lower

Table 7.
Results of ANOVA assessment for mean steady state absorption rate of CO_2 with main effects and interaction contributing over 95% towards the output response.

Source	DoF	Adj SS	Adj MS	F-Value	P-Value	Contribution (%)
EBRT[*]	1	229.965	229.965	97.45	<0.001	44.67
pH[*]	1	110.024	110.024	46.62	<0.001	21.37
L/G[*]	1	74.911	74.911	31.74	0.001	14.55
L/G *vs.* pH[*]	1	45.692	45.692	19.36	0.003	8.88
Alk	1	10.893	10.893	4.62	0.069	2.12
L/G *vs.* u_G	1	9.842	9.842	4.17	0.08	1.91
u_G *vs.* pH	1	8.773	8.773	3.72	0.095	1.70
u_G	1	8.159	8.159	3.46	0.105	1.58
Pooled error	7	16.519	2.36	-	-	3.21
Cumulative total	15	514.778	-	-	-	100.00

[*] Denotes the statistically significant ($P < 0.05$) source (factors).
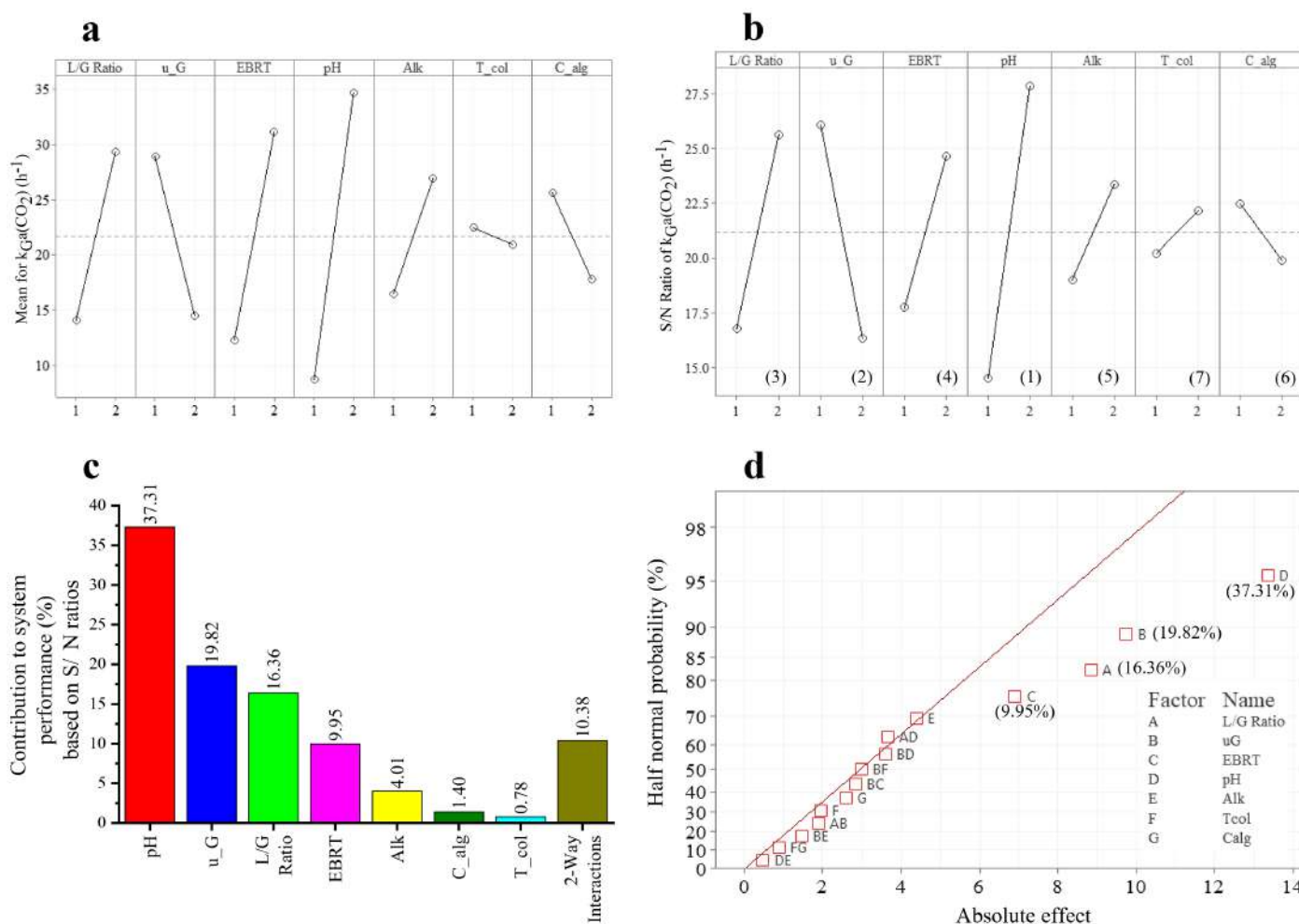
Fig. 8. Analysis plots for relative influence of design factors on the gas side volumetric mass transfer coefficient for CO_2: **(a)** Main effects plot with means; **(b)** Main effects plots with S/N ratio. The rank of each design factor is included in parenthesis; **(c)** Contribution of each design factor and interactions on the overall system outcome; and **(d)** Half normal probability plot with the relative contribution of major effects highlighted in brackets.

the hydrodynamic performance (a lower $k_{G_{CO_2}}a$, **Fig. 8a**) and its corresponding resilience (a lower S/N ratio, **Fig. 8b**). **Figure 8c** shows the relatively large contributions of pH (37.31%), superficial gas velocity (19.82%), L/G ratio (16.36%), and EBRT (9.55%) on the hydrodynamic parameter of $k_{G_{CO_2}}a$. However, although the contribution of alkalinity was substantial (over 4%, **Fig. 8c**), the half normal probability plot in **Figure 8d** indicated its weak influence on the mean overall CO_2 mass transfer coefficient (being located on the 45° line).

The pooled ANOVA presented in **Table 8** nonetheless confirmed the statistical significance ($P < 0.05$) of the influence of alkalinity, alongside those of pH, superficial gas velocity, L/G ratio and EBRT on the bubble column hydrodynamics with respect to CO_2 absorption. None of the other main effects and interactions caused any statistically significant ($P < 0.05$) variation on the current process response.

3.3.4. O_2 content in biomethane ($O_{2,\%,BM}$)

The L/G ratio had by far the largest influence among all other design factors on the O_2 content of the upgraded biomethane ($O_{2,\%,BM}$) (**Figs. 9a-d**) whereby, a higher setting of L/G ratio led to the increase of $O_{2,\%,BM}$. Besides L/G ratio, pH, EBRT, and algal concentration increased $O_{2,\%,BM}$ (a higher mean response, **Fig. 9a**) when operated at the higher setting ("2"). On the contrary, both temperature and alkalinity were found to lower $O_{2,\%,BM}$ when increased. The increase of $O_{2,\%,BM}$ from an increased superficial gas velocity was minimal. To achieve grid quality biomethane, the aim is to minimise oxygen stripping; however, an increase in the mean process response ($O_{2,\%,BM}$), would lower

Table 8.
Results of ANOVA assessment for mean overall CO_2 mass transfer coefficient with main effects and interaction contributing over 95% towards the output response.

Source	DoF	Adj SS	Adj MS	F-Value	P-Value	Contribution (%)
pH[*]	1	715.65	715.65	67.08	<0.001	37.31
u_G[*]	1	380.13	380.13	35.63	0.002	19.82
L/G[*]	1	313.79	313.79	29.41	0.003	16.36
EBRT[*]	1	190.91	190.91	17.89	0.008	9.95
Alk[*]	1	76.89	76.89	7.21	0.044	4.01
L/G *vs.* pH	1	53.39	53.39	5	0.075	2.78
u_G *vs.* pH	1	51.36	51.36	4.81	0.08	2.68
u_G *vs.* T_{col}	1	35.59	35.59	3.34	0.127	1.86
u_G *vs.* EBRT	1	32.13	32.13	3.01	0.143	1.68
T_{col}	1	15.01	15.01	1.41	0.289	0.78
Pooled error	5	53.34	10.67	-	-	2.78
Cumulative total	15	1918.19	-	-	-	100

[*] Denotes the statistically significant ($P < 0.05$) source (factors).
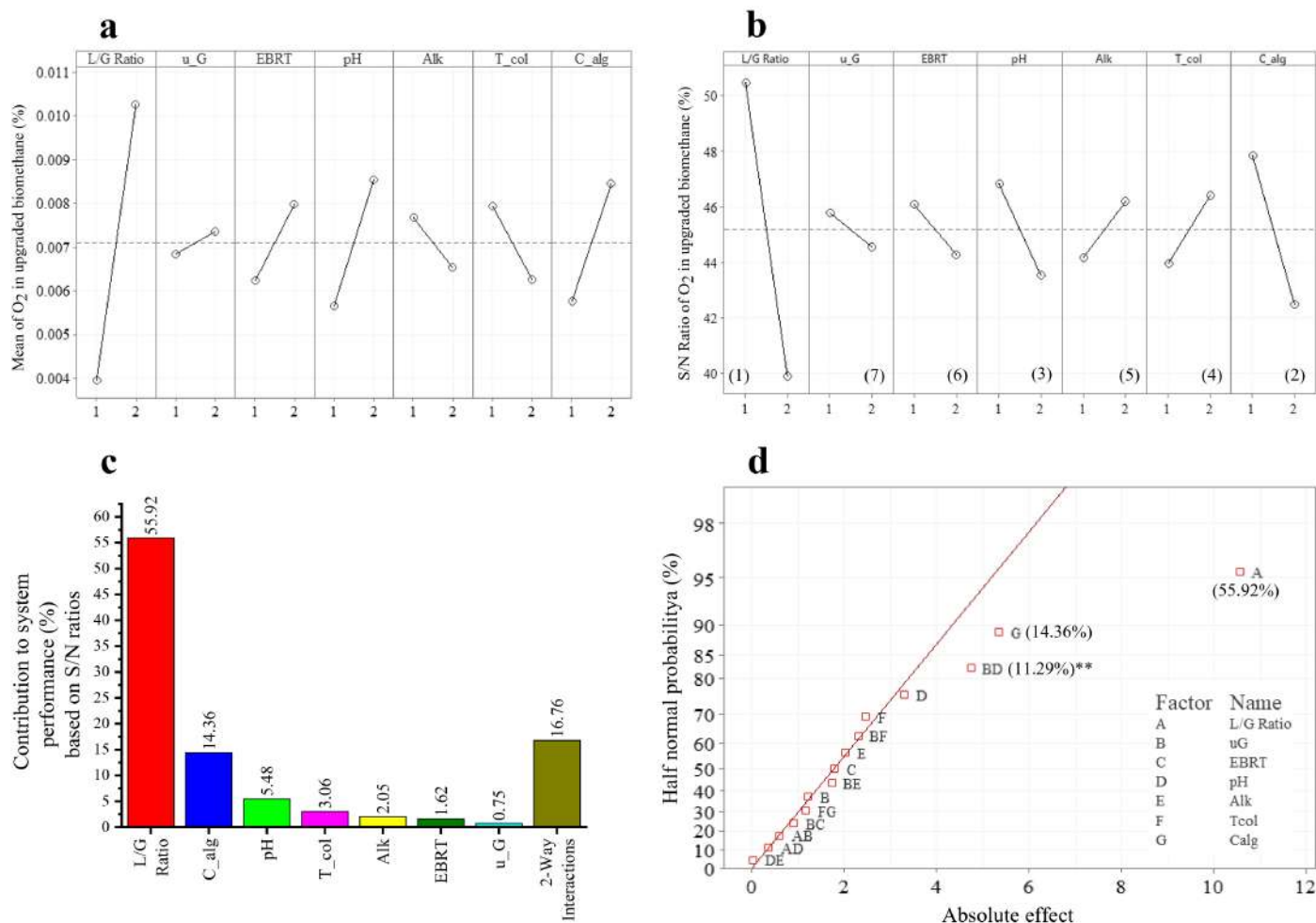
Fig. 9. Analysis plots for relative influence of design factors on O_2 concentration in biomethane: **(a)** Main effects plot with means; **(b)** Main effects plots with S/N ratio. The rank of each design factor is included in parenthesis; **(c)** Contribution of each design factor and interactions on the overall system outcome; and **(d)** Half normal probability plot with the relative contribution of major effects highlighted in brackets.

the robustness of operation. As a result, unlike the plots for CO_2, where the 'larger-the-better' response was desired, the main effects plot with S/N ratio for oxygen stripping had an opposite slope to that of the main effects plot with means. Accordingly, the factors such as L/G ratio that raised the mean response on their increase, resulted in the drop of S/N ratio for the same and *vice versa* (**Fig. 9b**). Following L/G ratio, algal concentration was the second most influential design factor, followed by pH. Numerically, they accounted for 55.92%, 14.36%, and 5.48% of the total variations in $O_{2,\%,BM}$ (**Fig. 9c**). All interactions combined caused 16.76% of the variations in the oxygen concentrations in biomethane.
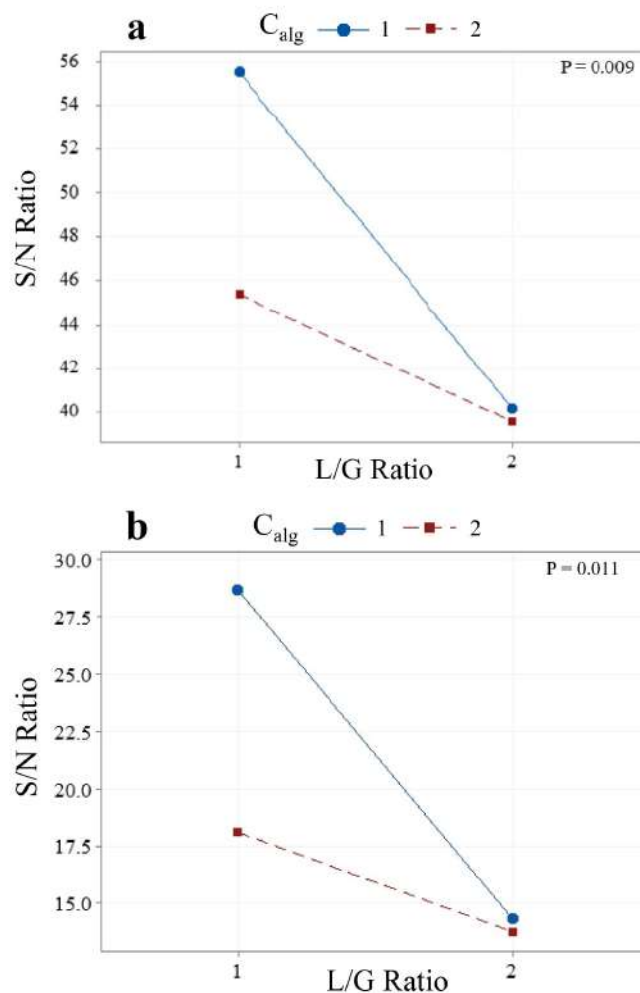
On further investigation into the half normal probability plot in **Figure 9d**, the interaction between superficial gas velocity and pH was obtained as the only major interaction (lying farthest from the 45° line). However, this is while the contribution of superficial gas velocity was not only low (0.75%, **Fig. 9c**) but it can also be seen to be lying over the 45° line in **Figure 9d**, indicating its weak statistical significance. To confirm this phenomenon, the pooled ANOVA was performed, including superficial gas velocity to maintain hierarchy. As can be seen from **Table 9**, while the influence of pH on the oxygen concentration in biomethane was statistically significant (P = 0.014), that of superficial gas velocity was not (P = 0.252). In contrast, their interaction showed a statistically significant effect (P = 0.003), contributing to over 11% in the variability of the current response (**Fig. 9d** and **Table 9**). This can be explained from the alias structure of the designed L_{16} OA, whereby the interactions between L/G and algal concentration were found to be confounded with the interactions between superficial gas velocity and pH and between EBRT and the bubble column temperature. To solve this issue, the hierarchical model was adopted, whereby the aliased effect can be assigned to the interaction that had both the main effects as statistically significant (P < 0.05) (Myers et al., 2017). Accordingly, the observed statistically significant (P < 0.05) interaction was concluded to be that between the two of the most impactful factors, L/G ratio and algal concentration (P < 0.001). The influence of temperature towards oxygen concentration in upgraded biomethane was also confirmed to be statistically significant (P < 0.05) *via* the pooled ANOVA (**Table 9**).

Figure 10a depicts the interactive effect between L/G ratio and the algal concentration on the $O_{2,\%,BM}$. A higher S/N ratio is always desired, as can be followed from **Figure 10a**, at a lower algal concentration (factor level "1"), L/G ratio is the primary influencer of oxygen stripping, with a higher L/G ratio signifying a higher $O_{2,\%,BM}$. At a higher algal concentration (factor level "2"), however, the relative variation in oxygen stripping between the extreme L/G

Fig. 10. Interaction between L/G ratio and algal concentration (C_{alg}) for **(a)** O_2 concentration in outlet biomethane and **(b)** O_2 outflow rate within upgraded biomethane.

ratios is considerably reduced. Especially at lower L/G ratios (factor level "1"), the increased presence of algae plays a major role in oxygen stripping (**Fig. 10a**), while at higher L/G ratios (factor level "2"), a comparable O_2 stripping leading to similar O_2 concentrations in biomethane can be noticed irrespective of the algal concentration. This indicates that although the hydrodynamics related to oxygen stripping are greatly affected by the increased presence of algae at lower L/G ratios, the effect diminishes largely at higher L/G ratios. A plausible explanation could be the relatively large influence of superficial liquid velocities on the system hydrodynamics, including bubble diameter and bubble rise velocity at higher liquid flow rates (Kulkarni and Joshi, 2005) (bubble column diameter being constant). Thus, at higher L/G ratios (factor level "2"), the ensuing biomethane would contain a high concentration of oxygen irrespective of the algal concentration in the circulating liquid.

3.3.5. O_2 outflow within biomethane ($O_{2,BM}$)

Opposite to that observed for $O_{2,\%,BM}$, **Figures 11a-d** reveals that the superficial gas velocity has the strongest proportional influence on the volume of oxygen stripped into the biogas per unit time ($O_{2,BM}$). The resulting increase of oxygen stripping would inherently cause a decreased performance of the bubble column, indicated by a corresponding drop in the S/N ratio on increasing the superficial gas velocity (**Fig. 11b**). This is

Table 9.
Results of ANOVA assessment for O_2 content in the upgraded biomethane with main effects and interaction contributing over 95% towards the output response.

Source	DoF	Adj SS	Adj MS	F-Value	p-Value	Contribution (%)
L/G ratio*	1	447.04	447.04	118.82	<0.001	55.92
C_{alg}*	1	114.808	114.808	30.51	0.001	14.36
u_G *vs.* pH*	1	90.228	90.228	23.98	0.003	11.29
pH*	1	43.779	43.779	11.64	0.014	5.48
T_{col}*	1	24.457	24.457	6.5	0.044	3.06
u_G *vs.* T_{col}	1	21.215	21.215	5.64	0.055	2.65
Alk	1	16.392	16.392	4.36	0.082	2.05
EBRT	1	12.963	12.963	3.45	0.113	1.62
u_G	1	6.031	6.031	1.6	0.252	0.75
Pooled error	6	22.575	3.762	-	-	2.82
Cumulative total	15	799.488	-	-	-	100

* Denotes the statistically significant (P < 0.05) source (factors).

Fig. 11. Analysis plots for relative influence of design factors on O_2 flow rate in biomethane: **(a)** Main effects plot with mean; **(b)** Main effects plots with S/N ratio. The rank of each design factor is included in parenthesis; **(c)** Contribution of each design factor and interactions on the overall system outcome; and **(d)** Half normal probability plot with the relative contribution of major effects highlighted in brackets.

followed in order by the influence of L/G ratio and algal concentration. EBRT and pH, on the other hand, were seen to only slightly increase the oxygen stripping, while alkalinity and temperature resulted in the lowering of the same (**Fig. 11a**). On the aspect of contribution, therefore, only superficial gas velocity (44.78%), L/G ratio (28.03%), and algal concentration (9.97%) affected oxygen stripping by more than 5% (**Fig. 11c**).

The confirmatory pooled ANOVA established the statistical significance (P < 0.05) of the three major design factors (superficial gas velocity, L/G ratio, and algal concentration in order) to impact on $O_{2,BM}$. Similar to $O_{2,\%,BM}$, a statistically significant (P = 0.004) interaction between superficial gas velocity and pH was obtained (seen as interaction BD, lying away from the 45° line in the half normal probability plot in **Figure 11d** and also confirmed by pooled ANOVA in **Table 10**). pH, however, had no statistically significant main effect (P = 0.231). By the hierarchical principle adopted above, the interaction was thus concluded to be that of the aliased interaction between the two statistically significant main effects, L/G ratio and algal concentration (P < 0.001). The interaction plot shown in **Figure 10b** shows a similar interactive effect to that of $O_{2,\%,BM}$.

3.4. Comparison between design factors and significant interactions

3.4.1. Main effects

Grid quality biomethane requires simultaneous maximisation of CO_2 removal and minimisation of O_2 stripping. As can be seen from **Table 11**, L/G

Table 10.
Results of ANOVA assessment for O_2 outflow with biomethane with main effects and interaction contributing over 90% towards the output response.

Source	DoF	Adj SS	Adj MS	F-Value	P-Value	Contribution (%)
u_G*	1	555.55	555.547	88.46	<0.001	44.78
L/G ratio*	1	347.78	347.778	55.38	<0.001	28.03
C_{alg}*	1	123.65	123.646	19.69	0.002	9.97
u_G *vs.* pH*	1	99.78	99.78	15.89	0.004	8.04
Alk	1	27.29	27.29	4.35	0.071	2.20
T_{col}	1	25.89	25.893	4.12	0.077	2.09
pH	1	10.55	10.551	1.68	0.231	0.85
Pooled error	8	50.24	6.28	-	-	4.05
Cumulative total	15	1240.72	-	-	-	100

* Denotes the statistically significant (P < 0.05) source (factors).

Table 11.
Comparison and primary conclusions about the design factors affecting the studied process responses to assess the performance of the bubble column in photosynthetic biogas upgrading for both CO_2 removal and O_2 stripping. The values in brackets indicate the rank of the design factors based on S/N ratios for the respective response. The arrows indicate the direction of the responses on increasing the setting of the design factors.

Design Factors	Performance of CO_2 removal			O_2 stripping		Inference
	R_{eff,CO_2} (%)	R_{abs,CO_2} ($\times 10^{-4}$ mol/L/s)	$k_{G_{CO_2}}a$ (h^{-1})	O_2 in biomethane (%)	O_2 outflow in biomethane (mL_n/min)	
L/G ratio	(2)* ↑	(3)* ↑	(3)* ↑	(1)* ↑	(2)* ↑	Critical influence
Superficial gas velocity	(5)* ↓	(6) ↓	(2)* ↓	(7) ↑	(1)* ↑	Minor influence
Empty bed residence time	(7) ↑	(1)* ↓	(4)* ↓	(6) ↑	(6) ↑	Negligible influence
pH of inlet liquid	(1)* ↑	(2)* ↑	(1)* ↑	(3)* ↑	(7) ↑	Critical influence
Alkalinity of inlet liquid	(3)* ↑	(4) ↑	(5) ↑	(5) ↓	(4) ↓	Major influence on CO_2 removal only
Temperature	(6) ↑	(6) ↑	(7) ↑	(4)* ↓	(5) ↓	Negligible influence
Algal concentration	(4)* ↓	(5) ↓	(6) ↓	(2)* ↑	(3)* ↑	Major influence on O_2 stripping only

* Indicates the statistically significant main effects (P < 0.05).

ratio is a critical design factor, having a major influence (within the top 3 factors) on each studied response. While a higher L/G ratio is desirable for better CO_2 removal, a lower L/G ratio would minimise both oxygen stripping and corresponding concentration in upgraded biomethane. This trend is similar to those reported in multiple literature sources (Toledo-Cervantes et al., 2017; Bose et al., 2019). pH is another critical design factor; a high pH would improve both the CO_2 absorption hydrodynamics and reaction rates, resulting in a consistent and robust CO_2 removal but would also increase O_2 stripping. Although this increase in O_2 stripping was not statistically significant (P = 0.231), the resulting increase in O_2 concentration in biomethane was (P = 0.014). This also validates the claim made by the authors in a previous study that a higher pH results in increased O_2 stripping (Bose et al., 2019). Thus, optimisation of the bubble column (not included in this work) must be performed with pH and L/G ratio as the most significant factors.

Higher algal concentration has a major influence on the $O_{2,\%,BM}$. It could be both due to the improved hydrodynamics and/or the transfer of a considerable amount of O_2 produced by photosynthesising microalgae into the biomethane. On the contrary, the absorption of CO_2 showed no statistically significant (P > 0.05) correlation with increasing algal concentration. However, the increased algal concentration resulted in a significant drop in the CO_2 removal efficiency of the bubble column. This could be because of non-uniform mixing due to the presence of filamentous microalgae (*S. platensis*), as well as from increased foaming and clogging observed at operations with higher algal concentrations. A similar drop in CO_2 removal efficiencies from increased algal concentration has also been reported by del Rosario Rodero et al. (2020b), although it was not statistically significant. Alkalinity was a major factor in R_{eff, CO_2} both increasing CO_2 removal and providing operation robustness when alkalinity was increased. A similar improvement in the consistency of R_{eff, CO_2} was reported by del Rosario Rodero et al. (2020b) by increasing the alkalinity from 1.3 gIC/L to 2.4 gIC/L and above. However, it had no major contribution to

either the kinetics or the hydrodynamics of CO_2 absorption, as well as on oxygen stripping.

Although superficial gas velocity plays a major role in defining the system hydrodynamics, it had a minor impact on the overall biomethane composition. In agreement with existing literature (Zedníková et al., 2018), superficial gas velocity had the highest influence on increasing the volume of O_2 stripped into the biogas. However, as the bubble column diameter was fixed, an increase in the superficial gas velocity was accompanied by a proportional increase in the gas flow rate. This ensured that there was no significant change in $O_{2,\%,BM}$ with the variation in the superficial gas velocity. From the perspective of CO_2 removal, a higher superficial gas velocity would not only increase bubble diameter but also increase the bubble rise velocity (Kulkarni and Joshi, 2005), decreasing the gas-liquid contact time irrespective of EBRT. Expectedly, all the metrics for CO_2 removal barring the CO_2 removal rate, showed a significant drop in performance on increasing the superficial gas velocity. However, it must be remembered that to increase the throughput of the bubble column with regards to biogas upgraded; the superficial gas velocity must be increased. Thus, to counter the drop in CO_2 removal performance with regards to increasing the superficial gas velocity, the operating pH, L/G ratio, and alkalinity must be included in process control and optimisation.

Compared to other design factors, the influence of temperature was minimal. Although $O_{2,\%,BM}$ had a statistically significant (P = 0.044) decrease upon the increase in the temperature, the net contribution of temperature towards the overall variation in the response was only around 2% (**Table 10**). Thus, the influence of temperature on the bubble column operations and controls can generally be neglected. Finally, beyond indicating a drop in reaction rates and hydrodynamic performance along the length of the reactor, which is expected from its co-current flow configuration, EBRT had no statistically significant contribution towards the upgraded biomethane composition and can hence be regarded as a minor factor when varied between 6 and 15 min. The major conclusions from the comparative assessment of the design factors on the design, operation, and control strategy of the bubble column for photosynthetic biogas upgrading are compiled in **Table 11**.

3.4.2. Interactions

A few interactive effects between the design factors were also found to have a major and statistically significant (P < 0.05) effect on the performance of CO_2 removal from biogas and O_2 stripping from the alkaline algal medium. For the former, the largest interaction was between pH and L/G ratio, affecting the rate of CO_2 absorption and hence the overall efficiency of CO_2 removal. The implications of the interactive effects between the superficial gas velocity and pH and L/G ratio imply the necessity to control both pH and L/G ratio at higher levels to enable an increase of the throughput of the bubble column (a higher gas superficial velocity for constant diameter). This is especially important, as the higher setting (factor level "2") of superficial gas velocity was limited by the practicality of the experimental setup. However, as both the upper levels (factor level "2") of pH and L/G were set at their maximum intended values, the conclusions of the present study would remain valid when the effect of higher superficial gas velocities is studied in future works. For O_2 stripping, the only statistically significant (P < 0.05) interaction was between algal concentration and L/G ratio. The results indicated the important influence of the algal concentration on increasing $O_{2,\%,BM}$ at a lower L/G ratio; however, at a higher L/G ratio, the $O_{2,\%,BM}$ was found to be independent of the algal concentration.

Of the interactive effects that were not statistically significant (P > 0.05), the interaction between temperature and algal concentration bears importance in that it provides conclusive evidence that the photosynthesising microalgae would not play a significant role in catalysing CO_2 removal. By this, it can also be confirmed that the absorption of CO_2 is chemically driven by the carbonate/bicarbonate present in the solution.

3.5. Prediction of bubble column operation and confirmatory experiment

Using the statistically significant (P < 0.05) main effects and interactions derived in *Section 3.3*, **Equations 15** and **16** were used to predict the CO_2

removal efficiency ($(S/N)_{R_{eff, CO_2}}$) and the oxygen outflow within biomethane ($(S/N)_{O_{2,BM}}$) in terms of the S/N ratio. For physical interpretation, the obtained values could be converted back into practical units using **Equations 10** and **11**, respectively.

$$(S/N)_{R_{eff, CO_2}} = \qquad\qquad\qquad\qquad \text{Eq. 15}$$
$$-53.25 + 56.69 L/G - 164.5 u_G + 5.04 pH + 1.1 Alk - 2.07 C_{alg} + 28.01 L/G * u_G$$
$$- 5.63 L/G * pH + 14.1 u_G * pH$$

$$(S/N)_{O_{2,BM}} = 44.13 - 18.79 L/G - 84.2 * u_G - 18.65 C_{alg} + 17.84 L/G * C_{alg} \qquad \text{Eq. 16}$$

To assess the performance of the derived regression models, their statistical characteristics were calculated and compared. As can be seen from the results summarised in **Table 12**, both the regression equations for R_{eff, CO_2} and $O_{2,BM}$ have a much higher F_{model} value (27.96 and 27.19, respectively) than critical values (3.725 and 3.36, respectively) with a P value of less than 0.001 in both cases. This confirms the statistical significance of the proposed regression models for a confidence interval of 95%. Simultaneously, the R^2 values of the models were also above 0.9, indicating a good linear agreement between the observed and the predicted data (Smith et al., 2016).

Table 12.
Statistical characteristics of the models for predicting CO_2 removal efficiency and O_2 flow rate in upgraded biomethane in order to predict the biomethane composition.

Model	Model Characteristics					
	DoF	R^2	S	F_{model}	$F_{critical}$	P-value
CO_2 removal efficiency	7	0.9697	1.11%	27.96	3.725 ($F_{0.05(8,7)}$)	<0.001
O_2 flow in biomethane	4	0.9081	3.22%	27.19	3.36 ($F_{0.05(5,10)}$)	<0.001

A study of the S value, which represents the average deviation of the predicted model from the observed data, shows that the model for R_{eff, CO_2} would be able to predict the performance based on S/N ratio with an average error of ± 1.11%; the corresponding average error in prediction of $O_{2,BM}$ is ± 3.22%. Graphical representation of this argument is presented in **Figure 12** that reveals a good agreement between the experimental and the predicted values for both S/N ratios of R_{eff, CO_2} and $O_{2,BM}$. All the experimental values were found to lie within the 95% prediction interval, confirming the adequacy of the simplified model with the chosen main effects and interactions.

A confirmatory experiment, separate from the sixteen Taguchi trials, was performed with pH 10.5 (to maximise CO_2 removal), L/G ratio 0.2 (to minimise O_2 stripping), and alkalinity 2.5 gIC/L (to maximise CO_2 removal efficiency) while the superficial gas velocity was set at 0.2 cm/s (to maximise throughput). The constant settings were selected as follows: temperature 20°C, algal concentration 0.05 g-DW/L, and EBRT 6 min. Grid quality biomethane with a CO_2 and O_2 concentration of 0.19% ± 0.17% and 0.2% ± 0.01%, respectively, was obtained. The corresponding S/N ratio for CO_2 removal efficiency of -0.0613 fell within the 95% CI of -2.28 and 1.66, while that for oxygen (20.77) matched closely with the predicted value of 22.78 while also being within the 95% CI (18.82, 23.74).

Following the predictive regression equations, **Figures 13a** and **b** represent the variation in biomethane composition between a pH 9 and pH 10.5 and an L/G ratio 0.2 and 1 for the superficial gas velocity of 0.06 cm/s (factor level "1") and 0.2 cm/s (factor level "2"), respectively. EBRT and temperature were set at the lowest ranges, while alkalinity was set at 2.5 gIC/L. Algal concentration was considered fixed at 0.05 g-DW/L. As can be seen, with the increase in superficial gas velocity, the allowable range of operation to produce grid quality biomethane narrows significantly, especially with respect to CO_2 removal. This can be understood from the interactive effect between superficial
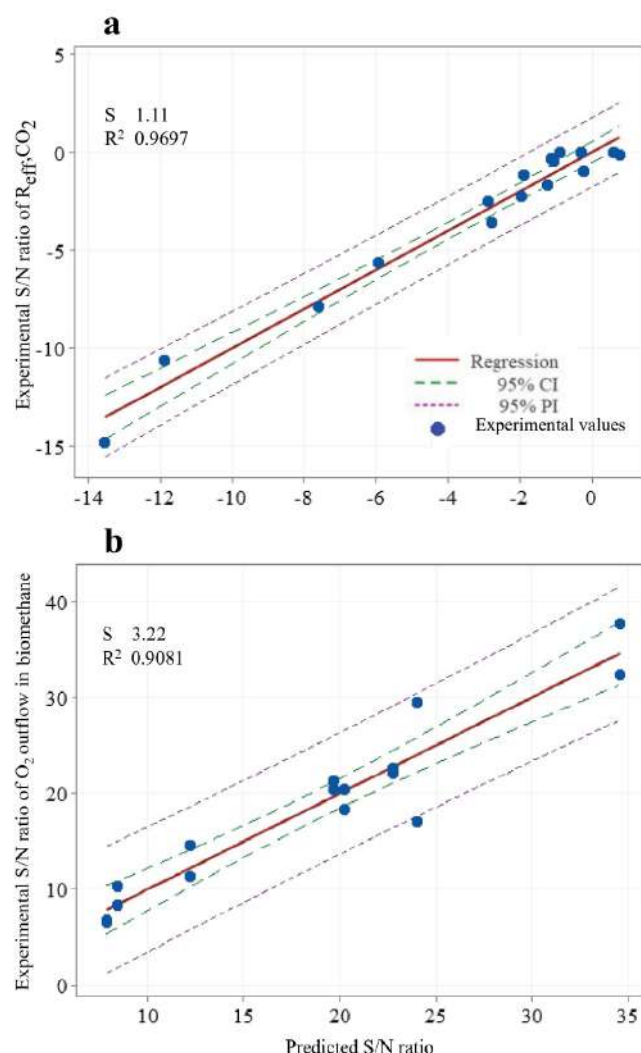
Fig. 12. Comparison of regression model and experimental data along with 95% Confidence Interval and 95% Prediction Interval for the S/N ratios of **(a)** R_{eff, CO_2} and **(b)** $O_{2,BM}$.

gas velocity and both pH and L/G ratio alike, whereby an increase in pH and L/G ratio was necessary at higher superficial gas velocity (throughput rates) to achieve grid quality biomethane, all other conditions being fixed.

Figure 13 must, however, be studied with caution as it is not an optimised plot, nor can it be extrapolated above the studied range of superficial gas velocity 0.2 cm/s. Indeed, this graph provides an indication and estimation of the profiles of biomethane composition to be expected while working with photosynthetic biogas upgrading. More accurate predictive models and contour plots must be generated with detailed optimisation experiments, which is beyond the scope of the present work.

3.6. Significance of results

Similar global hydrodynamic parameters, such as the gas hold-up (i.e., the ratio of the gassed volume to the static liquid volume in the bubble column), are necessary and sufficient to achieve dynamic similarity upon scale up (Shaikh and Al-Dahhan, 2010). For low superficial gas velocities below 1 cm/s, a minimal gas hold-up together with a negligible impact of pressure on the same allows scale-up of results with minimal errors (Bose et al., 2021). Accordingly, the current results would remain valid for industrial-scale bubble columns operated under similar superficial gas velocities irrespective of the bubble column dimensions. The following sections, therefore, focus on the significance of the results on the industrial
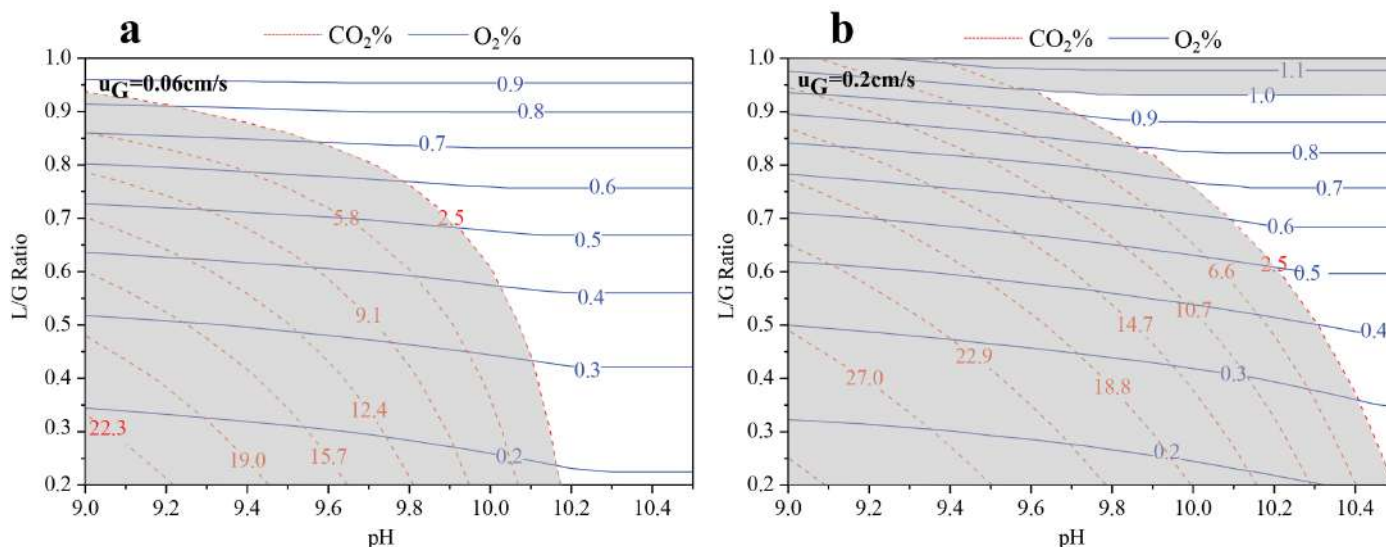
Fig. 13. Prediction of Biomethane composition at **(a)** u_G 0.06 cm/s (~0.98 L/h) and **(b)** u_G 0.2 cm/s (~3.29 L/h). The constant setting of other design factors are as follows: Alk 2.5gIC/L; T_{col} 20°C; C_{alg} 0.05g-DW/L; and EBRT 6 min. The acceptable region of operation is indicated in white.

scale design, operation, and costs of the bubble column, together with its integration with photobioreactors for the continuous operation of photosynthetic biogas upgrading system producing grid quality biomethane.

3.6.1. On bubble column design, operation, and costs

To ensure robust and repetitive operation of the bubble column, against uncontrollable factors or noise such as DO in the algal liquid or seasonal and diurnal cycles, process control strategies for bubble column operation must include L/G ratio and pH as critical factors along with alkalinity. The compelling evidence of the benefits of operation with a low algal concentration and the minor influence of temperature between 20 °C and 35 °C would further ease the design and operation of the bubble column. Not only does a lower algal concentration signify that light would not play a signify role in bubble column operations, but also that control of temperature and pressure are not crucial elements to its operation and control. From the bubble column design aspect, the relatively minor influence of EBRT as it varied between 6 and 15 min, indicates the possibility to reduce the height of the bubble column from that currently employed in literature for photosynthetic biogas upgrading. On the other hand, for a fixed bubble column diameter, to ensure a constant EBRT, the bubble column height would increase proportionally with the superficial gas velocity. Indeed, within the present experiments, this resulted in the aspect ratio (the ratio of the height of the bubble column to the diameter) to vary from 9 to 22.5 at superficial gas velocities of 0.06 cm/s and 0.2 cm/s, respectively, and an EBRT of 6 min. Thus, it can be concluded with confidence ($P < 0.05$) that biomethane production in photosynthetic biogas upgrading would be possible in industrial bubble columns with their aspect ratios typically varying between 3 and 10 (Jakobsen, 2009). Traditional materials such as stainless steel could be used for bubble column construction without the need for specialised design and materials. However, to further increase the superficial gas velocity without having to build a considerably tall bubble column, an investigation into lowering the EBRT further can be made in future studies. pH and alkalinity must be set to the maximum setting (10.5 and 2.5 g-IC/L, corresponding to factor level "2" in the present study), with the L/G being adjusted accordingly to ensure generation of grid quality biomethane.

3.6.2. On the operation of algae cultivation and harvesting system

From mass balance, the CO_2 removed from the biogas in the bubble column would be added into the alkaline algal liquid, increasing its alkalinity and producing bicarbonates from carbonates (**Eq. 1**). Based on the CO_2 removal efficiency, **Table 13** indicates the predicted effective amount of inorganic carbon added into the algal liquid from biogas in terms of alkalinity (g-IC/L). Operation at two extremes of pH and L/G ratios when the superficial gas velocity is 0.2 cm/s is considered as a representative case. A high pH and low L/G ratio, ensuring 96.5% CO_2 removal (predicted), would maximise the inorganic carbon addition per litre of alkaline solution. However, when the L/G ratio is increased to 1, IC added would drop to 0.2gIC/L at a CO_2 removal efficiency of 100%.

Table 13.
Statistical Impact of pH and L/G ratio on the inorganic carbon added to the algal liquid from biogas with the corresponding CO_2 removal efficiency in brackets. CO_2 removal efficiencies are based on the predicted values obtained using **Equations 15** and **10** in order.

pH	LG ratio	
	0.2	1
9	0.30 (30.1%)	0.17 (87.7%)
10.5	0.96 (96.5%)	0.20 (100%)

To ensure a continuous cycle, the added carbon must account for that consumed by the algae and also meet system losses. Carbon losses in closed and open pond photobioreactors have been reported to be similar (Bose et al., 2019), often increasing at higher alkalinity (del Rosario Rodero et al., 2020b). Assuming the average productivity of *S. platensis* in inorganic media to be around 0.175 g/L/d at 30 °C (De Oliveira et al., 1999), and that *S. platensis* comprises 50% carbon per dry weight (Binaghi et al., 2003), the daily carbon assimilation rate would be 0.088 g/L. Also, considering a carbon loss of 24% at an alkalinity of 2.5 gIC/L (del Rosario Rodero et al., 2020b), the cultivation of *S. platensis* at 30 °C, connected to a bubble column operating at pH 10.5 and L/G 0.2 would require an estimated 8 days of hydraulic retention time (HRT) to assimilate the added carbon. However, when the L/G ratio is increased to 1, the HRT could be reduced to 2 days only. The corresponding algal concentrations generated would vary between 2.8 gDW/L and 0.35 gDW/L, respectively. Sufficient year-round

CO_2 uptake could be ensured by temperature-controlled microalgae cultivation, either in closed photobioreactors (Bose et al., 2019) or open ponds within greenhouses (Marín et al., 2021). A higher algal concentration is always desired, as it greatly simplifies the harvesting system design and cost.

4. Conclusions and future directions

In this work, a quantitative comparison among seven design factors affecting bubble column performance in photosynthetic biogas upgrading has been developed. The L_{16} Taguchi OA as a screening design of experiment was selected as the statistical tool. Experiments were conducted in a lab-scale bubble column reactor. Assessments regarding the performance of CO_2 removal and O_2 stripping into biomethane were performed using the S/N ratio statistic derived from the experimental data. The output of the four objectives as described in the introduction along with future research needs are synthesised as below:

i.   pH and L/G ratio are the most critical design factors affecting CO_2 removal and O_2 stripping alike. For CO_2 removal in a specific bubble column, besides pH and L/G ratio, alkalinity, followed by algal concentration and superficial gas velocity are statistically significant ($P < 0.05$) design factors. On the other hand, over 90% of the variations in O_2 concentration in biomethane were explained by the main effects of L/G ratio, algal concentration, and pH (in descending order of importance).

ii. The interactive effect between pH and L/G ratio was the most impactful on the efficiency of CO_2 removal. Although superficial gas velocity had limited contribution to CO_2 removal, its interactions with both L/G ratio and pH caused statistically significant ($P < 0.05$) variation in the CO_2 composition in biomethane. For O_2 stripping, algal concentration had a diminishing role in increasing the O_2 concentration in biomethane as the L/G ratio increased. At higher L/G ratios, similar O_2 concentration in biomethane was observed irrespective of the algal concentration in the circulating algal medium.

iii. A higher alkalinity (2.5 gIC/L) is required to ensure consistent CO_2 removal while a lower algal concentration (0.05 gDW/L) would minimise O_2 stripping into biomethane, and also maximise and staibilise CO_2 removal. Although a high pH and L/G ratio improves CO_2 removal, it increases O_2 content in the biomethane. A higher superficial gas velocity, on the other hand, reduces the CO_2 removal efficiency without affecting the O_2 concentration in biomethane. Thus, future studies aiming to increase the throughput of the system and optimise the bubble column would require pH, L/G ratio, and superficial gas velocity as mandatory design factors.

iv. Using only the statistically significant main effects and interactions, the biomethane composition (CO_2% and O_2%) was predicted with fair confidence for superficial gas velocities up to 0.2 cm/s using regression equations derived from the ANOVA analysis. To achieve grid quality biomethane, operations at pH between 10.3 and 10.5 and L/G ratio between 0.5 and 0.8, with an alkalinity of 2.5 gIC/L and algal concentration of 0.05 gDW/L would ensure robust operations. However, to generate more accurate predictive models, detailed optimisation experiments with the selected critical design factors must be conducted; these were beyond the scope of the present work. The minimal impact of temperature and gas residence times on the system performance further indicates the possibility to use state-of-the-art bubble column designs and operational strategies for photosynthetic biogas upgrading.

Based on the results of the current work, the need to perform further research to examine increasing the superficial gas velocities and lowering the EBRT can be established. This would be essential to increase the throughput of the bubble columns without requiring them to be considerably tall. In all cases, however, pH, L/G ratio, and alkalinity must be varied taking into account the feasibility of integration with the photobioreactor for microalgae cultivation to achieve the optimal design and operating conditions of the bubble column.

References

[1]   American Public Health Association (APHA), 1992. APHA Method 2320, in: standard methods for the examination of water and wastewater. American Public Health Association (APHA), Washington, DC.

[2]   Angelidaki, I., Treu, L., Tsapekos, P., Luo, G., Campanaro, S., Wenzel, H., Kougias, P.G., 2018. Biogas upgrading and utilization: current status and perspectives. Biotechnol. Adv. 36(2), 452-466.

[3]   Antony, J., 2014. 4 - A systematic methodology for design of experiments, 2nd ed. Des. Exp. Eng. Sci. 33-50.

[4]   Awty-carroll, D., Ravella, S., Clifton-brown, J., Robson, P., 2020. Using a Taguchi DOE to investigate factors and interactions affecting germination in Miscanthus sinensis. Sci. Rep. 10(1), 1-11.

[5]   Bahr, M., Díaz, I., Dominguez, A., González Sánchez, A., Muñoz, R., 2014. Microalgal-biotechnology as a platform for an integral biogas upgrading and nutrient removal from anaerobic effluents. Environ. Sci. Technol. 48(1), 573-581.

[6]   Barros, A.I., Gonçalves, A.L., Simões, M., Pires, J.C., 2015. Harvesting techniques applied to microalgae : a review. Renew. Sustain. Energy Rev. 41, 1489-1500.

[7]   Binaghi, L., Del Borghi, A., Lodi, A., Converti, A., Del Borghi, M., 2003. Batch and fed-batch uptake of carbon dioxide by Spirulina platensis. Process Biochem. 38(9), 1341-1346.

[8]   Borhani, T.N.G., Azarpour, A., Akbari, V., Alwi, S.R.W., Manan, Z.A., 2015. CO_2 capture with potassium carbonate solutions: a state-of-the-art review. Int. J. Greenhouse Gas Control. 41, 142-162.

[9]   Bose, A., Lin, R., Rajendran, K., Xia, A., O'Shea, R., Murphy, J.D., 2019. How to optimize photosynthetic biogas upgrading: a perspective on system design and microalgae selection. Biotechnol. Adv. 37(8), 107444.

[10] Bose, A., O'Shea, R., Lin, R., Murphy, J.D., 2020. A perspective on novel cascading algal biomethane biorefinery systems. Bioresour. Technol. 304, 123027.

[11] Bose, A., O'Shea, R., Lin, R., Murphy, J.D., 2021. Design, commissioning and performance assessment of a lab-scale bubble column reactor for photosynthetic biogas upgrading with Spirulina platensis. Ind. Eng. Chem. Res. 60(15), 5688–5704.

[12] Chen, P.C., Huang, C.H., Su, T., Chen, H.W., Yang, M.W, Tsao, J.M., 2015. Optimum conditions for the capture of carbon dioxide with a bubble-column scrubber. Int. J. Greenhouse Gas Control. 35, 47-55.

[13] Chen, P.C., Lin, S., 2018. Optimization in the absorption and desorption of CO_2 using sodium glycinate solution. Appl. Sci. 8(11), 2041.

[14] Chiranjeevi, P., Mohan, S.V., 2016. Critical parametric influence on microalgae cultivation towards maximizing biomass growth with simultaneous lipid productivity. Renewable Energy. 98, 64-71.

[15] Clark, K.N., 1990. The effect of high pressure and temperature on phase distributions in a bubble column. Chem. Eng. Sci. 45(8), 2301-2307.

[16] Costa, J.A.V., Colla, L.M., Duarte Filho, P., 2003. Spirulina platensis growth in open raceway ponds using fresh water supplemented with carbon, nitrogen and metal ions. Z. Naturforsch. C. 58(1-2), 76-80.

[17] Davis, R., John, P., 2018. Application of Taguchi-Based Design of Experiments for Industrial Chemical Processes, in: Silva, V. (Ed.), Statistical Approaches With Emphasis on Design of Experiments Applied to Chemical Processes Montgomery. IntechOpen.

[18] Deckwer, W.D., Louisi, Y., Zaidi, A., Ralek, M., 1980. Hydrodynamic properties of the fischer-tropsch slurry process. Ind. Eng. Chem. Process Des. Dev. 19(4), 699-708.

[19] del Rosario Rodero, M., Carvajal, A., Castro, V., Navia, D., de Prada, C., Lebrero, R., Muñoz, R., 2019a. Development of a control strategy to cope with biogas flowrate variations during photosynthetic biogas upgrading. Biomass Bioenergy. 131, 105414.

[20] del Rosario Rodero, M., Lebrero, R., Serrano, E., Lara, E., Arbib, Z., García-Encina, P.A., Muñoz, R., 2019b. Technology validation of

photosynthetic biogas upgrading in a semi- industrial scale algal-bacterial photobioreactor. Bioresour. Technol. 279, 43-49.

[21] del Rosario Rodero, M., Carvajal, A., Arbib, Z., Lara, E., de Prada, C., Lebrero, R., Muñoz, R., 2020a. Performance evaluation of a control strategy for photosynthetic biogas upgrading in a semi-industrial scale photobioreactor. Bioresour. Technol. 307, 123207.

[22] del Rosario Rodero, M., Severi, C.A., Rocher-Rivas, R., Quijano, G., Muñoz, R., 2020b. Long-term influence of high alkalinity on the performance of photosynthetic biogas upgrading. Fuel. 281, 118804.

[23] del Rosario Rodero, M., Posadas, E., Toledo-Cervantes, A., Lebrero, R., Muñoz, R., 2018. Influence of alkalinity and temperature on photosynthetic biogas upgrading efficiency in high rate algal ponds. Algal Res. 33, 284-290.

[24] De Oliveira, M.A.C.L. Monteiro, M.P.C., Robbs, P.G., Leite, S.G.F., 1999. Growth and chemical composition of Spirulina maxima and Spirulina platensis biomass at different temperatures. Aquacult. Int. 7(4), 261-275.

[25] Fernández, I, Guzmán, J.L., Berenguel, M., Acién, F.G., 2017. Dynamic modeling of microalgal production in photobioreactors, in: tripathi, Bhumi Nath, Kumar, D. (Eds.), Prospects and Challenges in Algal Biotechnology. Springer, pp. 49-86.

[26] Franco-Morgado, M., Alcántara, C., Noyola, A., Muñoz, R., González-Sánchez, A., 2017. A study of photosynthetic biogas upgrading based on a high rate algal pond under alkaline conditions: influence of the illumination regime. Sci. Total Environ. 592, 419-425.

[27] Ganapathy, T., Murugesan, K.A., Gakkhar, R.P., 2009. Performance optimization of Jatropha biodiesel engine model using Taguchi approach. Appl. Energy. 86(11), 2476-2486.

[28] Gas Networks Ireland, 2018. Code of Operations, Part G.

[29] Hikita, H., Asai, S., Takatsuka, T., 1976. Absorption of carbon dioxide into aqueous sodium hydroxide and sodium carbonate-bicarbonate solutions. Chem. Eng. J. 11(2), 131-141.

[30] Hu, G., Nicholas, N.J., Smith, K.H., Mumford, K.A., Kentish, S.E., Stevens, G.W., 2016. Carbon dioxide absorption into promoted potassium carbonate solutions: a review. Int. J. Greenhouse Gas Control. 53, 28-40.

[31] Hu, Q., Guterman, H., Richmond, A., 1996. A flat inclined modular photobioreactor for outdoor mass cultivation of photoautotrophs. Biotechnol. Bioeng. 51(1), 51-60.

[32] Huang, Q., Jiang, F., Wang, L., Yang, C., 2017. Design of photobioreactors for mass cultivation of photosynthetic organisms. Engineering. 3(3), 318-329.

[33] Jakobsen, H.A., 2009. Bubble Column Reactors, in: Chemical Reactor Modeling, Multiphase Reactive Flows. Springer Berlin Heidelberg, Trondheim, pp. 335-501.

[34] Jones, B., 2016. 21st century screening experiments: what, why, and how. Qual. Eng. 28(1), 98-106.

[35] Kaye, G. W.C., Laby, T.H., 1986. Tables of physical and chemical constants and some mathematical functions, 15th Ed. London, New York, Longman.

[36] Kim, H.Y., 2017. Statistical notes for clinical researchers: chi-squared test and Fisher's exact test. Restor. Dent. Endod. 42(2), 152.

[37] Kishore, R.A., Kumar, P., Priya, S., 2018. A comprehensive optimization study on $Bi_2 Te_3$ -based thermoelectric generators using the Taguchi method. Sust. Energy Fuels. 2(1), 175-190.

[38] Kitchin, J., 1994. 6 - Basic statistical inference, in: dunning, F.B. (Ed.), Methods in Experimental Physics. Elsevier Masson SAS, Houston, Texas, pp. 28, 155-186.

[39] Knuutila, H., Juliussen, O., Svendsen, H.F., 2010. Kinetics of the reaction of carbon dioxide with aqueous sodium and potassium carbonate solutions. Chem. Eng. Sci. 65(23), 6077-6088.

[40] Krishnaiah, K., Shahabudeen, P., 2012. Applied Design of Experiments and Taguchi Methods. PHI Learning Private Limited, New Delhi.

[41] Kulkarni, A.A., Joshi, J.B., 2005. Bubble formation and bubble rise velocity in gas - liquid systems : a review. Ind. Eng. Chem. Res. 44(16), 5873-5931.

[42] Madkour, F.F., Kamil, A.E.W., Nasr, H.S., 2012. Production and nutritive value of Spirulina platensis in reduced cost media. Egypt. J. Aquat. Res. 38(1), 51-57.

[43] Marín, D., Carmona-Martínez, A.A., Blanco, S., Lebrero, R., Muñoz, R.,

[44] 2021. Innovative operational strategies in photosynthetic biogas upgrading in an outdoors pilot scale algal-bacterial photobioreactor. Chemosphere. 264(1), 128470.

[45] Marín, D., Posadas, E., Cano, P., Pérez, V., Blanco, S., Lebrero, R., Muñoz, R., 2018. Seasonal variation of biogas upgrading coupled with digestate treatment in an outdoors pilot scale algal-bacterial photobioreactor. Bioresour. Technol. 263, 58-66.

[45] Mehta, P.D., 2001. Control variable in research. Int. Encycl. Social Behav. Sci. 2727-2730.

[46] Meier, L., Barros, P., Torres, A., Vilchez, C., Jeison, D., 2017. Photosynthetic biogas upgrading using microalgae: effect of light/dark photoperiod. Renewable Energy. 106, 17-23.

[47] Meier, L., Martínez, C., Vílchez, C., Bernard, O., Jeison, D., 2019. Evaluation of the feasibility of photosynthetic biogas upgrading: Simulation of a large-scale system. Energy. 198, 116313.

[48] Meier, L., Pérez, R., Azócar, L., Rivas, M., Jeison, D., 2015. Photosynthetic CO_2 uptake by microalgae: an attractive tool for biogas upgrading. Biomass Bioenergy. 73, 102-109.

[49] Mohsin, I., He, K., Li, Z., Zhang, F., Du, R., 2020. Optimization of the polishing efficiency and torque by using Taguchi method and ANOVA in robotic polishing. Appl. Sci. 10(3), 824.

[50] Molina, E., Ferna, J., Acie, F.G., Chisti, Y., 2001. Tubular photobioreactor design for algal cultures. J. Biotechnol. 92(2), 113-131.

[51] Montgomery, D.C., 2012. Design and Analysis of Experiments, 9th ed. John Wiley and Sons, Inc.

[52] Myers, R.H., Montgomery, D.C., Anderson-Cook, C.M., 2017. Response surface methodology: process and product optimization using designed experiments, 4th ed. John Wiley & Sons Inc, New Jersey.

[53] Posadas, E., del Mar Morales, M., Gomez, C., Acién, F.G., Muñoz, R., 2015a. Influence of pH and CO_2 source on the performance of microalgae-based secondary domestic wastewater treatment in outdoors pilot raceways. Chem. Eng. J. 265, 239-248.

[54] Posadas, E., Serejo, M.L., Blanco, S., Pérez, R., García-Encina, P.A., Muñoz, R., 2015b. Minimization of biomethane oxygen concentration during biogas upgrading in algal-bacterial photobioreactors. Algal Res. 12, 221-229.

[55] Priyadarshi, D., Paul, K.K., 2019. Optimisation of biodiesel production using Taguchi model. Waste Biomass Valorization. 10(6), 1547-1559.

[56] Rajendran, K., O'Gallachoir, B., Murphy, J.D., 2019. The combined role of policy and incentives in promoting cost ef fi cient decarbonisation of energy : a case study for biomethane. J. Clean. Prod. 219, 278-290.

[57] Rao, R.S., Kumar, C.G., Prakasham, R.S., Hobbs, P.J., 2008. The Taguchi methodology as a statistical tool for biotechnological applications : a critical appraisal. Biotechnol. J. 3(4), 510-523.

[58] Roy, R.K., 2010. A primer on the Taguchi method, second edition. Society of Manufacturing Engineers.

[59] Shah, S.R., Parikh, R.H., Chavda, J.R., Sheth, N.R., 2013. Application of Plackett-Burman screening design for preparing glibenclamide nanoparticles for dissolution enhancement. Powder Technol. 235, 405-411.

[60] Singh, G., Patidar, S.K., 2018. Microalgae harvesting techniques: a review. J. Environ. Manage. 217, 499-508.

[61] Shaikh, A., Al-Dahhan, M., 2010. A new methodology for hydraulic similarity in bubble columns. Can. J. Chem. Eng. 88(4), 503-517.

[62] Smith, Z.D., Keller, J.R., Bello, M., Cordes, N.L., Welch, C.F., Torres, J.A., Goodwin, L.A., Pacheco, R.M., Sandoval, C.W., 2016. Plackett-Burman experimental design to facilitate syntactic foam development. J. Appl. Polym. Sci. 133(1).

[63] Sun, Z., Liu, J., Zhou, Z.G., 2016. Algae for biofuels: an emerging feedstock, in: Luque, R., Lin, C.S.K., Wilson, K., Clark, J. (Eds.), Handbook of Biofuels Production, 2nd ed. Elsevier, pp. 673-698.

[64] Toledo-Cervantes, A., Madrid-Chirinos, C., Cantera, S., Lebrero, R., Muñoz, R., 2017. Influence of the gas-liquid flow configuration in the absorption column on photosynthetic biogas upgrading in algal-bacterial photobioreactors. Bioresour. Technol. 225, 336-342.

[65] Vasumathi, K.K., Premalatha, M., Subramanian, P., 2012. Parameters influencing the design of photobioreactor for the growth of microalgae. Renew. Sust. Energy Rev. 16(7), 5443-5450.

[66] Wall, D.M., McDonagh, S., Murphy, J.D., 2017. Cascading biomethane energy systems for sustainable green gas production in a circular economy. Bioresour. Technol. 243, 1207-1215.

[67] Yang, J., Cui, X., Feng, Y., Jing, G., Kang, L., Luo, M., 2017. Experimental study on microalgae cultivation in novel photobioreactor of concentric double tubes with aeration pores along tube length direction. Int. J. Green Energy. 14(15), 1269-1276.

[68] Zedníková, M., Orvalho, S., Fialová, M., Ruzicka, M.C., 2018. Measurement of volumetric mass transfer coefficient in bubble columns. ChemEngineering 2(2), 19.

Dr. Richard O'Shea is a lecturer in the Science Foundation Ireland MaREI centre based in the Environmental Research Institute in University College Cork, Ireland. Dr. O'Shea received a Ph.D. in Energy Engineering from University College Cork in 2018. He has published 34 research articles in the academic press with an h-index of 15 and over 600 citations. His current research interests are anaerobic digestion, sustainability, multicriteria decision analysis, technoeconomic analysis, and decarbonization of the food and beverage industry. His Google Scholar profile can be found at the following link: https://scholar.google.com/citations?user=dGm5ysAAAAAJ&hl=en.

Prof. Jerry Murphy serves as the Director of the SFI funded MaREI centre for energy, climate, and marine, as Professor Chair of Civil Engineering at UCC, and as Leader of the Biogas Task at International Energy Agency (IEA) Bioenergy. He has authored and edited numerous IEA Bioenergy reports. He serves on the advisory board of a number of international organisations, including DBFZ (German Bioenergy Research Centre). He has authored over 160 peer-review journal papers and is listed in the top 2% of cited academics worldwide. His research profile is available at http://orcid.org/0000-0003-2120-1357.

Dr. Richen Lin is a lecturer in the Science Foundation Ireland MaREI centre headquartered in the Environmental Research Institute in University College Cork, Ireland. He has a Ph.D. degree in Energy and Environmental Engineering from Zhejiang University, China, in 2016. He was a previous Marie Skłodowska-Curie Fellow (2018-2020) with a research focus on microbial electron transfer in anaerobic digestion. He has published over 50 peer-reviewed journal papers with an h-index of 23 and over 1700 citations. His research interests include (1) bio/electrochemical CO_2 valorisation; (2) cascading circular bio-based systems; and (3) negative carbon emission technologies, such as pyrochar. His research profile on Google Scholar can be found at the following link: https://scholar.google.com/citations?user=otyeO6QAAAAJ&hl=en.

Archishman Bose is a Ph.D. researcher at the Bioenergy and Biofuels Research Group within the Science Foundation Ireland MaREI centre headquartered in the Environmental Research Institute in University College Cork, Ireland. He has a dual Master's degree in Energy Engineering from KTH Royal Institute of Technology, Sweden and Politecnico di Torino, Italy and a Bachelor`s Degree in Mechanical Engineering from Jadavpur University, India. He has previously published over 10 peer-reviewed journal papers with an h-index of 6 covering a wide range of subjects within sustainable energy. His research interests include (1) novel biogas upgrading technologies; (2) microalgal systems; (3) circular and bioeconomy systems; and (4) techno-economic and sustainability analysis of energy systems. His research profile on Google Scholar can be found at the following link: https://scholar.google.com/citations?user=DT5wyDIAAAAJ&hl=en.